28. Gillespie JS. The rat anococcygeus muscle; a new, densely innervated smooth muscle preparation. Br J Pharmacol 43:430 (1971).

29. Larson BA, Gibson A, Bern HA. The effects of urotensins in tetrapods: physiology or pharmacology? In: Neurosecretion and the Biology of Neuropeptides (Kobayashi H, Bern HA, Urano A, eds). Tokyo:Japan Scientific Society Press, 1985;486-493.

30. Gibson A, Bern HA, Ginsburg M, Botting JH. Neuropeptide-induced contraction and relaxation of the mouse anococcygeus muscle. Proc Natl Acad Sci USA 81:625-629 (1984).

31. Tobin C, Joubert Y. Testosterone-induced development of rat levator ani muscle. Dev Biol 146: 131-138 (1991).

32. Guglielmone R, Vercelli A. The costo-uterine muscle of the rat. Anat Embryol 184:337-343 (1991).

33. Gibson A, Gillespie JS. The effect of immunosympathectomy and of 6-hydroxydopamine on the responses of the rat anococcygeus to nerve stimulation and to some drugs. Br J Pharmacol 47:261-267 (1973).

34. Fukazawa Y, Suzuki A, Iguchi T, Takasugi N, Bern HA. Sexual dimorphism and strain difference in mouse anococcygeus muscle. Zool Sci 9:1273 (1992).

Last Update: September 18, 1998

Hormones and Behavior 40, 248–251 (2001)
doi:10.1006/hbeh.2001.1675, available online at http://www.idealibrary.com on IDEAL®

Developmental Effects of Estrogenic Agents on Mice, Fish, and Frogs: A Mini-Review

Taisen Iguchi, Hajime Watanabe, and Yoshinao Katsu

Center for Integrative Bioscience, Okazaki National Research Institutes, 38 Nishigonaka, Myodaiji, Okazaki 444-8585, Japan; and CREST, Japan Science and Technology Corporation, 4-1-8 Honmachi, Kawaguchi 332-0012, Japan

Received August 9, 2000; accepted March 1, 2001

Laboratory experiments have demonstrated that exposure of rodents to sex hormones during prenatal or early postnatal life can cause permanent and irreversible alterations of the endocrine and reproductive organs, such as ovary, fallopian tube, uterus, cervix, vagina, and mammary gland in females; and testis, epididymis, prostate, and seminal vesicle in males; as well as non reproductive organs including bones and muscle and immune and nervous systems in both sexes. Early development of *Xenopus laevis* into the tadpole and *Fundulus heteroclitus* goes through a rapid cell division, gastrulation, neurulation, and organogenesis within 1 week after fertilization. The developing embryo is very fragile and sensitive to estrogenic agents. Thus, these animals can be used as a suitable model for examining the effect of endocrine disruptors (hormonally active agents) on the development of aquatic living beings, which are most likely to be exposed to the compounds. © 2001 Academic Press

Key Words: **mouse; frog; fish; developmental effects; estrogen; diethylstilbestrol; bisphenol A; nonylphenol; dioxins; PCBs.**

HORMONALLY ACTIVE CHEMICALS IN RIVER WATER AND DIOXINS IN WILDLIFE IN JAPAN

In order to study possible effects of hormonally active agents on developing animals, study of chemical contamination in the environment is needed. The Japanese government has been monitoring hormonally active chemicals in the river water and dioxins in wildlife. The Ministry of Construction measured levels of eight chemicals, such as bisphenol-A (BPA), nonylphenol (NP), octylphenols, phthalates, and 17β-estradiol (E_2) in 261 locations in 109 rivers. BPA (up to 0.64 μg/l) was found in ca. 40% of locations; E_2 (up to 13 ng/l) was found in 75% of locations; NP (up to 3.3 μg/l) in 13% of locations; and di(2-ethylhexyl)phthalate (DEHP) (up to 2.4 μg/l) in 25% of locations in 1999. Concentrations of these chemicals were lower (ca. 50%) as compared to those found in 1998, except for NP. These chemicals were degraded by sewage treatment; however, E_2 was found in the effluent. In the sediment, NP (up to 2700 μg/kg in 80% of locations), DEHP (up to 2900 μg/kg in 90% of locations), BPA (up to 89 μg/kg in 85% of locations), and E_2 (up to 1.2 μg/kg in 45% of locations) were found in 1999.

We have recently found that titanium-oxide- (TiO_2) fixed photocatalysts could completely abolish estrogenic activity of 10^{-7} M E_2 in water as assayed by a yeast system transfected with human estrogen receptor-α (ERα) (Kubota *et al.*, 1999). The same treatment also abolished estrogenic activity of BPA dissolved in water. We need further study to detect whether chemicals are degraded and to understand the inactivation mechanism of estrogenic action of chemicals by TiO_2.

The Environment Agency Japan measured dioxins in marine mammals, birds, raccoon dogs, and field mice in 1999. Dioxins (pg TEQ/g fat) were found in whales (*Mesoplodon stejnegeri*) (52–360 pg), finless dolphins (*Phocoenoides dalli*) (7.6–240 pg), kites (*Milvus lineatus*) (110–5400 pg), cormorants (*Phalacrocorax carbo*) (1200–9900 pg), field mice (*Apodemus speciosus*) (3.8–110 pg), and raccoon dogs (*Nyctereutes procynoides*) (23–660 pg). Dioxins levels were higher in birds living in urban areas than in rural areas.

PERINATAL MOUSE (*Mus musculus*) MODEL

Perinatal sex-hormone exposure has been found to induce lesions reproductive tracts in female mice

0018-506X/01 $35.00

(Takasugi, 1976; Takasugi and Bern, 1988). The possible relevance of the mouse findings to the development of cancer in humans has been emphasized (Bern, 1992; Iguchi, 1992, 2000; Iguchi and Bern, 1996). In the early 1970s, it was demonstrated that a close correlation exists between occurrence of vaginal clear cell carcinoma in young women and early intrauterine exposure to diethylstilbestrol (DES) (Herbst and Bern, 1981). Many chemicals released into the environment potentially disrupt the endocrine system in wildlife and humans, some of which have estrogenic activity by binding to the ERα. The neonatal mouse model has been utilized especially to demonstrate the long-term effects of early sex-hormone exposure on the female reproductive tract. Neonatal treatment of female mice with estrogens induces various abnormalities in the reproductive tract; ovary-independent cervicovaginal keratinization, adenosis, and tumors; uterine hypoplasia, epithelial metaplasia and tumors; oviducal tumors; and polyovular follicles and polyfollicular ovaries. The growth response of neonatally DES-exposed reproductive organs to estrogen is reduced, as are ERα levels, EGF receptor levels, along with other hormone receptor levels. The utility of the neonatal mouse model in indicating permanent, long-term changes, both overt and cryptic, in a variety of structures, both reproductive and nonreproductive, is emphasized, with particular attention herein to newer information of estrogens on ERα expression, oncogene expression, ovarian abnormalities, fertilizability, and skeletal and muscular tissues (Iguchi and Sato, 2000).

BPA can be found in canned drinks up to 213 ppb (Kawamura *et al.*, 1999) and in river water in Japan as described above. BPA and other chemicals, such as dioxins (10 fg/g wet wt), PCBs, DDTs, BHC, cadmium (100 pg), lead (10 ng), BPA, and NP (100 ng) were found in the human umbilical cord (Takada *et al.*, 1998; Mori, in press). Therefore, transplacental transfer of BPA was studied using the pregnant ICR/Jcl mouse and Japanese monkey (*Macaca fuscata*). BPA was found in fetal mouse serum, liver, brain, testis, and uterus within 30 min and in fetal monkey serum, brain, and liver within 1 h after BPA exposure to the mothers (Uchida *et al.*, unpublished data).

In utero exposure to BPA (300 μg/30 g BW) and DES (0.2 and 2 μg/30 g BW) reduced ovulatory activity in mice at 40 days of age. Only 2 μg DES induced ovary-independent vaginal stratification and uterine metaplasia. BPA-exposed (300 and 3000 μg) and 0.02 μg DES-exposed females gave birth when mated with untreated males, and the number of pups and sex ratio were not different from those of controls (Suzuki *et al.*, 1999). Howdeshell *et al.* (1999) demonstrated that exposure to BPA (2.4 μg/kg BW) *in utero* advances puberty and increases body weight in female offspring. Gupta (2000) also showed that mice fed with DES (100 ng/kg/day), BPA (50 μg/kg/day), and aroclor 1016 (50 μg/kg/day) had enhanced anogenital distance, increased prostate size, decreased epididymal weight, and increased androgen receptor binding activity of the prostate. Gupta (2000) showed enlargement of prostate size by *in vitro* DES exposure using organ culture system; therefore, *in vivo* experiments were reproduced in the *in vitro* experiment. We recently found that DES (0.02–2 μg/kg BW) and BPA (20 μg/kg BW) from days 11–17 of pregnancy accelerated vaginal opening but not body weight gain in mice (Honma *et al.*, unpublished data). Neonatal exposure to a high dose of BPA (150 μg per pup), but not 15 μg BPA, induced ovary-independent vaginal changes, uterine metaplasia, and polyovular follicles and infertility due to lack of a corpora lutea (Suzuki *et al.*, 1999). Female hypospadias, the formation of a common canal due to the fusion between the vagina and urethra with a wide cleft clitoris, can be induced in female mice when estrogen and androgen were given to newborn mice (Iguchi, 1992). The lowest dose of DES in induction of the hypospadias was 0.03 μg/pup and the critical period for DES exposure was 7 days after birth in female mice; however, BPA did not induce hypospadias in newborn mice (Miyakawa *et al.*, unpublished data). Thus, the developing organism is sensitive to exposure to estrogenic agents in the induction of long-term changes in reproductive organs during the critical period.

FISH MODEL

In *Fundulus heteroclitus*, for embryos reared in seawater containing 10^{-10}, 10^{-8}, and 10^{-6} M E_2, hatching and survival rates decreased in a dose-dependent manner, and fry treated with 10^{-6} and 10^{-8} M E_2 were dead by 2 and 12 weeks after hatching, respectively. More than 85% of fry treated with 10^{-8} M E_2 showed malformations 8 weeks after hatching (Urushitani *et al.*, 1997). Ossification was not completed in vertebrae, cranial bones, and other bones in fry treated with 10^{-8} M E_2 even 12 weeks after hatching. The sex ratio of control fry was 57% male and 43% female, whereas fry treated with 10^{-8} M E_2 were 100% female 8 weeks after hatching. Vitellogenin (VTG) mRNA was expressed in male liver by exposure to BPA, NP, or E_2 (Urushitani *et al.*, 2000). These data suggest that estrogen can in-

duce sex change and malformation in developing fish embryos and expression of VTG mRNA in male liver can be used as a marker of estrogenic activity of chemicals.

In order to study the molecular mechanism of estrogenic chemicals on developing fish, DNA sequences of ER and SF1/FTZ are essential. Therefore, the cDNA fragment was cloned from *F. heteroclitus* and contained 1536 nucleotides encoding 511 amino acid residues belonging to the ERα group and shared 86% identity to that of medaka (*Oryzias lapites*). Northern blot analysis showed that the 4.6-kb mRNA was strongly induced by exposure to E_2 in liver. These results indicated that the cDNA cloned from female liver RNA is the partial sequence of the ERα. Urushitani *et al.* (unpublished data) cloned a fragment of SF1/FTZ gene, which expressed strongly in the ovary, since SF1 is essential for mammalian gonad formation (Luo *et al.*, 1994).

Reproductive ability was studied in medaka exposed to estrogenic chemicals for 2 weeks (Shioda and Wakabayashi, 2000). They reported that exposure to E_2 (3 nM) caused a significant decrease in the number of eggs and hatchings as compared to the control group. The highest concentrations of BPA (10 μM) and NP (0.3 μM) caused a decrease in the number of hatchings, but no decrease in hatchings was observed in DEHP-exposed animals, even at 1 μM. These results suggest only estrogenic chemicals have adverse effect on development of medaka, since DEHP has no estrogenic activity in *in vitro* assay using MCF-7 cells and yeast transfected with human ERα (Harris *et al.*, 1997).

FROG MODEL

Xenopus laevis embryos were grown from developmental stage 3 in water containing 10^{-10}, 10^{-9}, 10^{-7}, 10^{-6}, and 10^{-5} M E_2, 17α-estradiol, or DES or 10^{-5} M progesterone (P) or dihydrotestosterone (DHT). Survival rates of the embryos developed in water containing 10^{-10}–10^{-6} M E_2 or DES, all concentrations of 17α-estradiol, and in water containing 10^{-5} M P or DHT were over 70% after stage 48, whereas the rates of the embryos treated with 10^{-5} M E_2 and DES decreased remarkably after stage 27 and all embryos were dead by stages 42 and 32, respectively. Embryos treated with 10^{-5} M E_2 showed malformations and suppressed organogenesis, including crooked vertebrae at stage 38; the head was smaller and the abdomen was larger than those in the controls. Similar effects were observed in embryos developed in 10^{-5} M DES, but not in 10^{-5} M 17α-estradiol, P, or DHT. In 10^{-5} M E_2 treatment, abnormalities were induced only when the treatment was started before stage 39. However, on the 30th day after fertilization, the size of the embryos treated with 10^{-6} M E_2 was larger than the controls. mRNA expression of ER (ER3 and ER4) genes were examined in eggs, embryos, and adult female liver by RT-PCR. ER4 was expressed in adult liver, unfertilized and fertilized eggs, and embryos. ER mRNA in 10^{-6} and 10^{-5} M E_2-treated embryos showed different expression patterns, which may be due to the diverse developmental effects of E_2. The present results indicate that 10^{-5} M E_2 and DES induced embryo death and malformations, and ER may be involved in the induction of the developmental defects in *Xenopus* embryos (Nishimura *et al.*, 1997).

Organochlorine compounds such as *o,p'*-DDT can mimic estrogen effects. Premature female color pattern induction in reed frog (*Hyperolius argus*) is specific to estrogens. Animals were treated at forelimb emergence and maintained in treated solution until final evaluation. E_2, *o,p'*-DDT (0.1 μg/l), *o,p'*-DDE (1 μg/l), and *o,p'*-DDD (1 μg/l) permanently induced adult female coloration pattern in juvenile animals, whereas *p,p'*-DDT, *p,p'*-DDE, and *p,p'*-DDD did not (Noriega and Hayes, 2000).

Frogs and toads do not usually drink water, but take water only through ventral skin. We found that male frogs absorb more water than female frogs. Water absorption through ventral skin is stimulated by vasotocin (VT). In frogs, the neurohypophysial hormones VT and mesotocin (MT) have an antidiuretic and a diuretic effect, respectively. However, a VT receptor (VR) has not been cloned and the effect of MT and sex steroids on water absorption through skin is still unclear. In addition, the frog population has been decreasing in the world, although the cause of the decline has not been clarified. Therefore, possible effects of endocrine disruption on the physiology of amphibians should be investigated.

We examined the effects of E_2, testosterone propionate (TP), BPA, and methoxychlor (Mx) on water absorption through ventral skin and cloned cDNAs for VR and MT receptor (MR) from the Japanese tree frog, *Hyla arborea japonica*, and identified their expressions in skin. In the control group male frogs absorbed more water than females. This sex difference disappeared after a single injection of E_2, BPA, and Mx. Water absorption increased only in females, but not in males after TP injection. Mx dissolved in water also lowered water absorption in females. We cloned two types of cDNAs, and their deduced amino acid se-

quences were similar to those of mammalian V_2R and toad MR, respectively. VR mRNA expression was more intense in ventral skin than in the dorsal skin. MR mRNA expression was more intense in dorsal skin than the ventral skin (Kohno *et al.*, 2000). Environmental estrogenic agents possibly affect water absorption in frogs.

CONCLUSIONS

The action of environmental estrogenic agents (pesticides, herbicides, polychlorinated compounds, plasticizers, and alkylphenols) during embryonic and fetal development demands extensive attention. As these effects may result in structural, reproductive, endocrinological, metabolic, immunological, neurological, behavioral, dysplastic, and neoplastic changes (Guillette and Crain, 2000), the search for the conseqences on the embryonic exposure must be stringent. Analyses of transgenerational effects of xenobiotic agents are needed in order to allow potential dangers to human and wildlife populations to be estimated and confronted.

ACKNOWLEDGMENTS

Supported by grants from Ministry of Education, Culture and Science of Japan.

REFERENCES

Bern, H. A. (1992). The fragile fetus. *In* T. Colborn and C. Clement. (Eds.), *Chemically-Induced Alterations in Sexual and Functional Development: The Wildlife/Human Connection*, pp. 9-15. Princeton Science, Princeton, NJ.

Guillette, L., Jr., and Crain, D. A. (Eds.) (2000). *Environmental Endocrine Disrupters—An Evolutionary Perspective.* Taylor & Francis, New York.

Gupta, C. (2000). Reproductive malformation of the male offspring following maternal exposure to estrogenic chemicals. *Proc. Soc. Exp. Biol. Med.* **224**, 61-68.

Harris, C. A., Henttu, P., Parker, M. G., and Sumpter, J. P. (1997). The estrogenic activity of phthalates *in vitro. Environ. Health Perspect.* **105**, 802-811.

Herbst, A. L., and Bern, H. A. (Eds.) (1981). *Developmental Effects of Diethylstilbestrol (DES) in Pregnancy.* Thieme Stratton, New York.

Howdeshell, K. L., Hotchkiss, A. K., Tayer, K. A., Vandenbergh, J. G., and vom Saal, F. S. (1999). Exposure to bisphenol A advances puberty. *Nature* **401**, 763-764.

Iguchi, T. (1992). Cellular effects of early exposure to sex hormones and antihormones. *Int. Rev. Cytol.* **139**, 1-57.

Iguchi, T. (2000). Embryonic and neonatal exposure to endocrine-altering contaminants: Effects on mammalian female reproduction. *In* Guillette, L., Jr. and D. A. Crain (Eds.), *Environmental Endocrine Disrupters*, pp. 234-268. Taylor & Francis, New York.

Iguchi, T., and Bern, H. A. (1996). Transgenerational effects: Intrauterine exposure to diethylstilbestrol (DES) in humans and the neonatal mouse model. *Comments Toxicol.* **5**, 367-380.

Iguchi, T., and Sato, T. (2000). Endocrine disruption and developmental abnormalities of female reproduction. *Am. Zool.* **40**, 402-411.

Kawamura, Y., Sano, H., and Yamada, T. (1999). Migration of bisphenol A from can coatings to drinks. *J. Food Hyg. Soc. Jpn.* **40**, 158-165.

Kohno, S., Kamishima, Y., and Iguchi, T. (2000). Sexual dimophic in ventral skin water absorption of Japanese tree frog (*Hyla jponica*). *In 25th Annual Meeting for Comparative Endocrinology*, Abstract 60, at Noto.

Kubota, Y., Niwa, C., Ohnuma, T., Nakajima, T., Iguchi, T., Hashimoto, K., Watabe, T., and Fujishima, A. (1999). Decomposition of estradiol by TiO_2 photocatalysis. *Light Technol. Front.* Nov. 26.

Luo, X., Ikeda, Y., and Parker, K. L. (1994). A cell-specific nuclear receptor is essential for adrenal and gonadal development and sexual differentiation. *Cell* **77**, 481-490.

Mori, C. (in press). Possible effects of endocrine disruptors on male reproductive function: A mini review. *Acta Anat. Nippon.*

Nishimura, N., Fukazawa, Y., Uchiyama, H., and Iguchi, T. (1997). Effects of estrogenic hormones on early development of *Xenopus laevis. J. Exp. Zool.* **278**, 221-233.

Noriega, N. C., and Hayes, T. B. (2000). DDT congener effects on secondary sex coloration in the reed frog *Hyperolius argus:* A partial evaluation of the *Hyperolius argus* endocrine screen. *Comp. Biochem. Physiol. B* **126**, 231-237.

Shioda, T., and Wakabayashi, M. (2000). Effect of certain chemicals on the reproduction of medaka (*Oryzias latipes*). *Chemosphere* **40**, 239-243.

Suzuki, A., Sugihara, A., and Iguchi, T. (1999). Developmental effects of diethylstilbestrol and bisphenol-A on reproductive organs in female mice. Abstract of 2nd Annual Meeting of Japan Society of Endocrine Disruptor Research, Kobe.

Takada, H., Isobe, T., Nakata, N., Nishiyama, H., Iguchi, T., Irie, H., and Mori, C. (1998). Detection of bisphenol A and nonylphenols in umbilical cords. Abstract of 1st Annual Meeting of Japan Society of Endocrine Disruptor Research, Kyoto.

Takasugi, N. (1976). Cytological basis for permanent vaginal changes in mice treated neonatally with steroid hormones. *Int. Rev. Cytol.* **44**, 193-224.

Takasugi, N., and Bern, H. A. (1988). Introduction: Abnormal genital tract development in mammals following early exposure to sex hormones. *In* T. Mori and H. Nagasawa (Eds.), *Toxicology of Hormones in Perinatal Life*, pp. 1-7. CRC Press, Boca Raton, FL.

Urushitani, H., Shimizu, A., Fukazawa, Y., Sato, T., and Iguchi, T. (1997). Developmental effect on gonadal differentiation and bones in *Fundulus heteroclitus. In* S. Kawashima and S. Kikuyama (Eds.), *Advances in Comparative Endocrinology*, pp. 311-315.

Urushitani, H., Sato, T., and Iguchi, T. (2000). Cloning and expression of estrogen receptor mRNA in mummichog, *Fundulus heteroclitus.* Abstract 15, 25th Annual Meeting for Comparative Endocrinology at Noto.

Brief Definitive Report

Dendritic Cell Maturation Overrules H-2D–mediated Natural Killer T (NKT) Cell Inhibition: Critical Role for B7 in CD1d-dependent NKT Cell Interferon γ Production

Yoshinori Ikarashi,[1] Rumiko Mikami,[1] Albert Bendelac,[2] Magali Terme,[1] Nathalie Chaput,[1] Masahiro Terada,[4] Thomas Tursz,[1] Eric Angevin,[1] François A. Lemonnier,[3] Hiro Wakasugi,[4] and Laurence Zitvogel[1]

[1]*Unité d'Immunologie, Département de Biologie Clinique, Institut Gustave Roussy, 94805 Villejuif Cedex, France*
[2]*Princeton University, Princeton, NJ 08544*
[3]*Unité d'Immunologie Cellulaire Antivirale, Institut Pasteur, Paris 75015, France*
[4]*Pharmacology Division, National Cancer Center, Tokyo 104-0045, Japan*

Abstract

Given the broad expression of H-2 class Ib molecules on hematopoietic cells, antigen presentation pathways among CD1d expressing cells might tightly regulate CD1d-restricted natural killer T (NKT) cells. Bone marrow–derived dendritic cells (BM-DCs) and not adherent splenocytes become capable of triggering $NK1.1^+$/T cell receptor $(TCR)^{int}$ hepatic NKT cell activation when (a) immature BM-DCs lack $H\text{-}2D^{b-/-}$ molecules or (b) BM-DCs undergo a stress signal of activation. In such conditions, BM-DCs promote T helper type 1 predominant CD1d-restricted NKT cell stimulation. H-2 class Ia–mediated inhibition involves more the direct $H\text{-}2D^b$ presentation than the indirect $Qa\text{-}1^b$ pathway. Such inhibition can be overruled by B7/CD28 interactions and marginally by CD40/CD40L or interleukin 12. These data point to a unique regulatory role of DCs in NKT cell innate immune responses and suggest that H-2 class Ia and Ib pathways differentially control NKT cell recognition of DC antigens.

Key words: inhibitory receptors • IFN-γ • costimulation • CD1d • NKT cells

Introduction

NKT cells are a recently described subpopulation of $TCR\alpha/\beta^+CD4^+$ or $CD4^-CD8^-$ T cells that have distinctive phenotypic and functional properties (1, 2). These T cells were first identified in mice, where they can be distinguished from conventional T cells by their expression of the NK locus-encoded C type lectin molecule NK1.1. Another hallmark of murine NKT cells is their extremely restricted TCR repertoire, with the great majority expressing an invariant TCRα chain structure (Vα14-Jα281) paired preferentially with Vβ8, 7, or 2. Both mouse and human NKT cells rapidly secrete cytokines associated with both Th1 (IFN-γ) or Th2 (IL-4) responses upon TCR engagement (1, 2) or stimulation with the synthetic CD1d ligand, the α-Galactosylceramide (α-GalCer) (3–5).

Recent results suggest a major role for murine NKT cells in the rejection of malignant tumors (6–10) and in regulating autoimmunity (11) and defense against certain pathogens. Indeed, NKT cells were shown to be relevant in innate antitumor immunosurveillance after IL-12 (6, 9) or α-GalCer administration (10, 12) but also in spontaneous, endogenous IL-12–dependent tumor models in mice (8). Cytokines play an important part at the NKT cell effector phase (8, 12). However, several conditions exist in which the apparent Th0 profile of cytokine production may be skewed toward a predominance of IFN-γ (11, 12) or IL-4 (13, 14) and IL-13 (15) leading to immunosuppression.

The origin and identity of the natural antigens recognized by CD1d-restricted T cells remain unknown. Given the canonical α chains and limited β chain diversity of the TCR of NKT cells, mCD1d may recognize a single or conserved set of antigens. Whether CD1d binding sphingolipid or phospholipid compounds represent self or foreign antigens (16), and whether the NKT cells responding

Y. Ikarashi and R. Mikami contributed equally to this work.
Address correspondence to Dr. Laurence Zitvogel, Unité d'Immunologie, Département de Biologie Clinique, (+12) Institut Gustave Roussy 39, rue Camille Desmoulins, 94805 Villejuif, France. Phone: 33-1-42-11-50-41; Fax: 33-1-42-11-60-94; E-mail: zitvogel@igr.fr

 J. Exp. Med. © The Rockefeller University Press • 0022-1007/2001/10/1179/08 $5.00
Volume 194, Number 8, October 15, 2001 1179–1186
http://www.jem.org/cgi/content/full/194/8/1179

to the synthetic α-GalCer are the same as those seeing phospholipids is unclear. However, mCD1d-restricted T cells varied in their recognition of different mCD1d transfected tumor cells suggesting that antigens presented by mCD1d molecules differ according to the cell type (17, 18). Variations in CD1d-restricted antigen presentation could arise from differences in expression, trafficking, processing, or loading of antigens (19).

As dendritic cells (DCs) are cornerstones between innate (20) and cognate immune responses, we investigated the regulatory mechanisms underlying the DC/NKT cell cross-talk in vitro. Our data imply that potent H-2D^b–mediated inhibition constitutively prevents DC-mediated IFN-γ production from resting NKT cells. The direct H-2D molecular pathway is partially involved in H-2 class I–mediated inhibition. However, after stress-induced maturation, DCs become electively capable of triggering CD1d-restricted NKT cells toward a Th1 predominant pattern in a B7/CD28-dependent manner, thereby overcoming H-2 class I–mediated inhibitory pathways. Our results provide further evidence for the pivotal role of DCs in NKT cell immune responses and identify DCs as a potential source of endogenous CD1d-restricted antigens.

Materials and Methods

Mice. Female C57BL/6 (H-2^b) mice were obtained from the Centre d' Elevage Janvier (Le Genest St Isle, France), the Centre d' Elevage Iffa Credo (L'Arbresle, France), and maintained in our animal facilities according to the Animal Experimental Ethics Committee Guidelines. Single H-2K$^{b-/-}$ and H-2D$^{b-/-}$ and double H-2K$^{b-/-}$D$^{b-/-}$ knockout (KO) mice as well as triple β2microglobulin$^{-/-}$H-2K$^{b-/-}$D$^{b-/-}$ KO mice were generated as described previously (21), bred in the animal facility of Institut Pasteur, and used at the sixth backcross generation onto C57BL/6 mice. CD1d$^{-/-}$ single and CD1d$^{-/-}$H-2K$^{b-/-}$D$^{b-/-}$ triple KO mice were generated as described previously (22), bred at Princeton Animal Facility or Pasteur Institute, and used at the seventh backcross generation onto C57BL/6 mice. All female mice were used at 6–25 wk of age.

Purification of Hepatic NKT Cells and T Cells. Hepatic NKT cells (defined as NK1.1$^+$TCR-β^{int} cells) and T cells (NK1.1$^-$ TCR-β^{high} cells) were prepared as described previously (23, 24). Briefly, hepatic mononuclear cells were stained with FITC-conjugated TCRβ (H57–597; BD PharMingen) and PE-conjugated NK1.1 (PK-136; BD PharMingen) and sorted by FACSVantage™ (Becton Dickinson). Purity of sorted cells exceeded 95% (data not shown). After overnight culture in complete medium, NKT cells could be restained using the anti-CD94 mAb coupled to PE (BD PharMingen).

Generation of DCs. Bone marrow (BM)-derived DCs (BM-DCs) were propagated from BM progenitor cells in culture medium supplemented with 1,000 IU/ml of rmGM-CSF (R&D Systems) and 1,000 IU/ml of rmIL-4 (R&D Systems) as described previously (20). Culture medium was renewed at day 2 and 4. To induce stress and maturation of DCs, day 6 DCs were harvested, spun down, and transferred into new 6-well plates (referred to as "transferred" henceforth). For phenotypic analyses, cells were preincubated with culture supernatant of hybridoma (2.4G2) secreting anti-CD16/CD32 mAb, and were subsequently incubated with FITC-conjugated anti-I-A^b (AF6-120.1) and PE-conjugated anti-CD11c (HL-3), FITC-conjugated CD80 (16–10A1), CD86 (GL1), CD40 (3/23) or PE-conjugated CD1d (1B1) or the anti-H2D^b (B22.249.R19; from H. Lemke, Institüt Für Genetik, Köln, Germany) or anti-H-2K^b (AF6–88.5.3 from American Type Culture Collection [HB-158]) mAb. All antibodies except 2.4G2 were purchased from BD PharMingen. Cells were gated according to size and granulosity with exclusion of PI-positive cells. Residual B lymphocytes (B220$^+$ cells) and granulocytes (Gr1$^+$ cells) were detected in the CD11c$^-$/I-A^{b-} cells and constitute <20% of whole cell population. T and NK cells were not propagated in these DC culture conditions. BM-DCs derived from gene targeted mice were analyzed for MHC class Ia and Ib expression and exhibited levels of MHC class II, CD80, CD86, CD40 expression comparable to those of wild-type (wt) BM-DCs (see Fig. 1, and data not shown). Splenic adherent cells were generated by subjecting red blood cell deprived splenocytes to 3 h adherence at 37°C. Adherent cells were rinsed three times with PBS, incubated with 10 mM EDTA for 20 min, and analyzed in FACScan™ for CD11c, MHC class II, CD1d, CD40, CD80, or CD86 expression.

In Vitro Cocultures. The hepatic NK1.1$^+$TCR-β^{int} NKT cells or NK1.1$^-$TCR-β^{high} T cells (5×10^4) were cocultured with immature or mature BM-DCs (2×10^3–10^4–5×10^4) in 200 μl of complete medium in 96-well U-bottomed plates for 24–44 h at 37°C, 5% CO_2. As positive controls, DCs were pulsed with 10 ng/ml of α-GalCer (provided by Pharmaceutical Research Laboratories, KIRIN Brewery Co., Gunma, Japan), washed in PBS, and cocultured with NKT cells. For blocking experiments, BM-DCs and NKT cells were cocultured in the presence of 50 μg/ml of neutralizing anti-CD40L mAb (MR; BD PharMingen), 50 μg/ml of CTLA-4 Ig fusion protein (gift from the Genetics Institute, Cambridge, MA), 25 μg/ml of anti–IL-12 mAb (C17.8; BD PharMingen), and of isotype-matched rat or hamster mAb (BD PharMingen). To mimic the stimulatory effects of B7 on mature DCs, we incubated immature day 6 BM-DCs with NKT cells along with 10 or 50 μg/ml of stimulating anti-CD28 mAb PV.1 (provided by C. June, University of Pennsylvania, Philadelphia, PA) plus or minus 100 IU rhIL-2/ml. To investigate the inhibitory pathways, immature DCs derived from wt mice were incubated with neutralizing anti-H2D^b (B22.249.R19; from H. Lemke, Köln, Germany) or anti-H-2K^b (AF6–88.5.3 from American Type Culture Collection [HB-158]) mAb and immature DCs derived from D$^{b-/-}$ mice were incubated with increasing dosages (1–5–10 μM) of Qdm1 (Qa-1^b binding peptide i.e. AMAPRTLLL) or R5K (mock Qa-1^b binding peptide i.e. AMVPKTLLL provided by D. Raulet, University of Berkeley, Berkeley, CA) peptides for 24 h at 37°C. The Qa-1^b mAb (clone 6A8.6F10.1A6) was purchased from BD PharMingen. All coculture conditions were performed in duplicates and experiments performed at least three times.

Cytokine Detection and Quantification (mIFNγ and mIL-4). After 20–44 h DC/NKT or T coculture, supernatants were harvested, stored at −80°C, and assessed either directly or after 5–50 times dilution using commercial ELISA kits (OptEIATM ELISA kit; BD PharMingen). The sensitivity of the mIFNγ kit was >31.5 pg/ml and that of mIL-4 kit was >7.15 pg/ml.

Statistical Analyses of Cytokine Levels. Fisher's exact method was used to compare means ± SE of IFN-γ production in-between various culture conditions and significant differences at 95% confidence are depicted with * on each graph.

Results and Discussion

Constitutive Inhibition of the DC/NKT Cell Cross-Talk. We first investigated the capacity of ex vivo propagated BM-DCs at an immature stage of differentiation to trigger cytokine secretion from resting hepatic NK1.1$^+$/TCR^{int} NKT cells in vitro. After 6 d of in vitro culture in GM-CSF plus IL-4, 50–55% BM cells became CD11c$^+$/MHC class II$^+$, expressed CD1d, and a small fraction was MHC class II^{bright} and expressed CD80, CD86, and CD40 molecules ("non transferred DC (day6)," Fig. 1). Such immature DCs, when cocultured with liver NKT cells at various DC/NKT cell ratios, did not induce NKT cell triggering as already reported (3, 12, 23; Fig. 2, a–c). Similar data were achieved using immature DCs propagated in GM-CSF alone or DCs sorted from spleens of Flt3L-treated mice (data not shown). As reported previously (23), when immature CD1d$^+$ DCs were pulsed with α-GalCer (1–10 ng/ml), high levels of IFN-γ (Fig. 3 a) and IL-4 (not shown) were measured in the supernatants of DC/NKT cell cocultures.

However, when derived from H-2D$^{b-/-}$K$^{b-/-}$ class I gene-targeted mice, immature DCs became capable of triggering IFN-γ secretion at nanogramm levels from hepatic NKT cells in a dose-dependent manner (Fig. 2 a). In contrast, low levels of IL-4 (100–300 pg/ml) were detected in the supernatants of NKT cells cocultured with H-2D$^{b-/-}$K$^{b-/-}$ gene-targeted BM-DCs (not shown). However, such nanogram levels of IFN-γ secretion were not found using BM-DCs propagated from H-2D$^{b-/-}$K$^{b-/-}$β2microglobulin$^{-/-}$ triple KO mice instead of D$^{b-/-}$K$^{b-/-}$ double KO mice (Fig. 2 a) suggesting that the constitutive

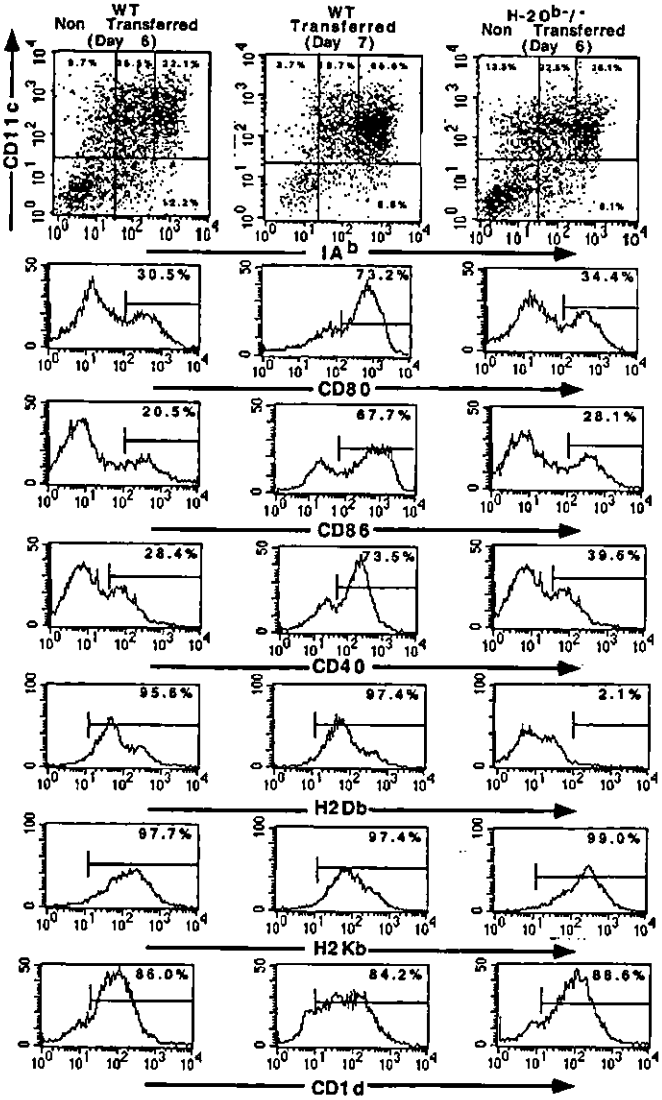

Figure 1. Phenotypic analyses of ex vivo propagated BM-DCs. BM-DCs (GM-CSF plus IL-4) at day 6 (wt, left panels, and H-2Db$^{-/-}$, right panels) before/or at day 7 after harvesting and transfer into new wells (wt, middle panels) were subjected to two color staining (CD11c-PE and I-A^b-FITC) or one-color staining (CD1d-PE and CD40, CD80, CD86-FITC, indirect staining for H-2D^b and H-2K^b expression) and immunostained cells were analyzed in flow cytometry.

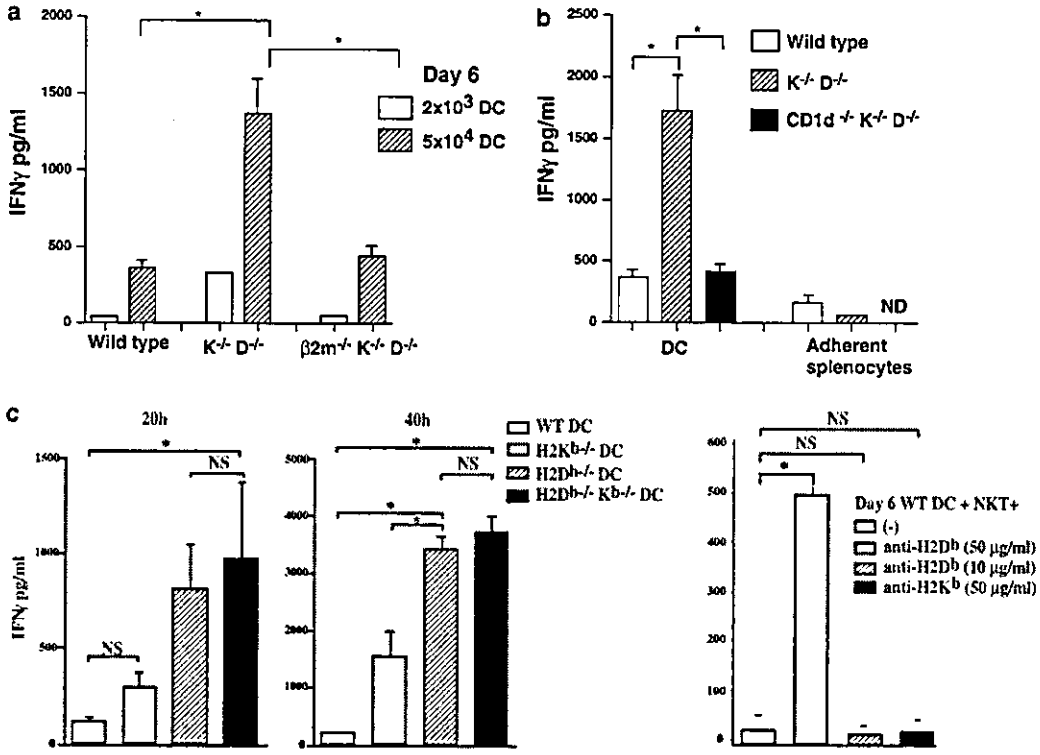

Figure 2. Constitutive H-2D–mediated NKT cell inhibition by immature DCs. (a) Day 6 immature BM-DCs derived from B6.wt or H-2K$^{b-/-}$D$^{b-/-}$ double KO or H-2K$^{b-/-}$D$^{b-/-}$β2m$^{-/-}$triple KO mice cocultured at a DC/NKT cell ratio of 1:1 or 1:25 with cell sorted hepatic NK1.1$^+$/TCR^{int} NKT cells for 40 h. (b) Similar experiments were performed comparing BM-DCs with adherent splenocytes derived from B6. wt versus H-2K$^{b-/-}$D$^{b-/-}$ double KO versus CD1d$^{-/-}$ K$^{b-/-}$ D$^{b-/-}$ triple KO mice cocultured with NKT cells at a DC/NKT cell ratio of 1:1 for 40 h. (c) Similar experiments were performed comparing immature day 6 BM-DCs derived from single (H-2K$^{b-/-}$ or H-2D$^{b-/-}$) KO mice versus H-2 K$^{b-/-}$D$^{b-/-}$ double KO mice (left panels). 24 and 40 h supernatants were assayed for IFN-γ in ELISA. Right panel depicts IFN-γ levels in the supernatants of NKT cells with day 6 wt BM-DCs incubated with increasing amounts of neutralizing Ab anti-H-2D^b or H-2K^b. Means ± SE are depicted in all graphs. Each graph represents either pooled data from three experiments performed in duplicate wells or a representative experiment out of three. Significant differences at 95% confidence using Fisher's exact method are outlined with *. All experiments were performed with KO female mice of 6–8 wk of age after 6–8 backcrosses on C57BL/6 mice. Phenotypic features were comparable in all gene targeted BM-DCs except for H-2 or CD1d molecule expression.

DC/NKT cell cross-talk involves β2microglobulin-associated H-2 class Ib molecules.

The DC/NKT Cell Cross-Talk Is Dependent on CD1d Molecules. We formally demonstrated that CD1d play a dominant role in the constitutive DC/NKT cell cross-talk by comparing IFN-γ levels secreted by NKT cells in coculture with BM-DCs derived from H-2D$^{b-/-}$K$^{b-/-}$ CD1d$^{-/-}$ versus H-2D$^{b-/-}$K$^{b-/-}$ mice originating from similar backcrosses in B6 mice (Fig. 2 b). DCs were electively endowed with the constitutive capacity to present CD1d-restricted antigens since CD1d$^+$/CD86$^+$/I-A^{b+} adherent splenocytes did not promote IFN-γ secretion from NKT cells even when derived from H-2D$^{b-/-}$K$^{b-/-}$mice (Fig. 2 b).

Direct Role of H-2D Molecules in the Constitutive Inhibition of the DC/NKT Cell Cross-Talk. It has been shown that NKT cell maturation is accompanied by extinction of Ly49 receptor expression. Liver NKT cells, as opposed to thymus NKT cells, are mature NKT cells and do not express Ly-49A, Ly-49C/I, or Ly-49-G (25). However, Skold and Cardell (26) pointed out the differential regulation of Ly49 expression on CD4$^+$ and double negative NK1.1$^+$ T cells with dramatic organ specific variations, stressing the complexity of NKT cell inhibitory pathways. Importantly, we were able to exclude a role for the H-2K^b/Ly49C pathway in the constitutive DC/NKT cell inhibition and to show a dominant inhibitory role of H-2D^b molecules at early time points of the DC/NKT cell interaction (Fig. 2 c, left panel). Searching for the H-2 D^b–specific inhibitory ligand, one should consider the possibility that H-2D^b recognition could be direct and/or indirect. Indirect recognition is possible via the ubiquitously expressed Qa-1^b molecules which preferentially associate with a H-2D^b leader peptide (Qdm), this peptide representing ~70% of those eluted from Qa-1 molecules (27, 28). A CD94-NKG2A NKT cell inhibition would not rule out the coexistence of an additional inhibitory receptor interacting directly with H-2D^b molecules. Therefore, we assessed the role of these inhibitory pathways by either (a) pulsing Qa-1b binding peptides (i.e. Qdm1 AMAPRTLLL or the mock peptides R5K

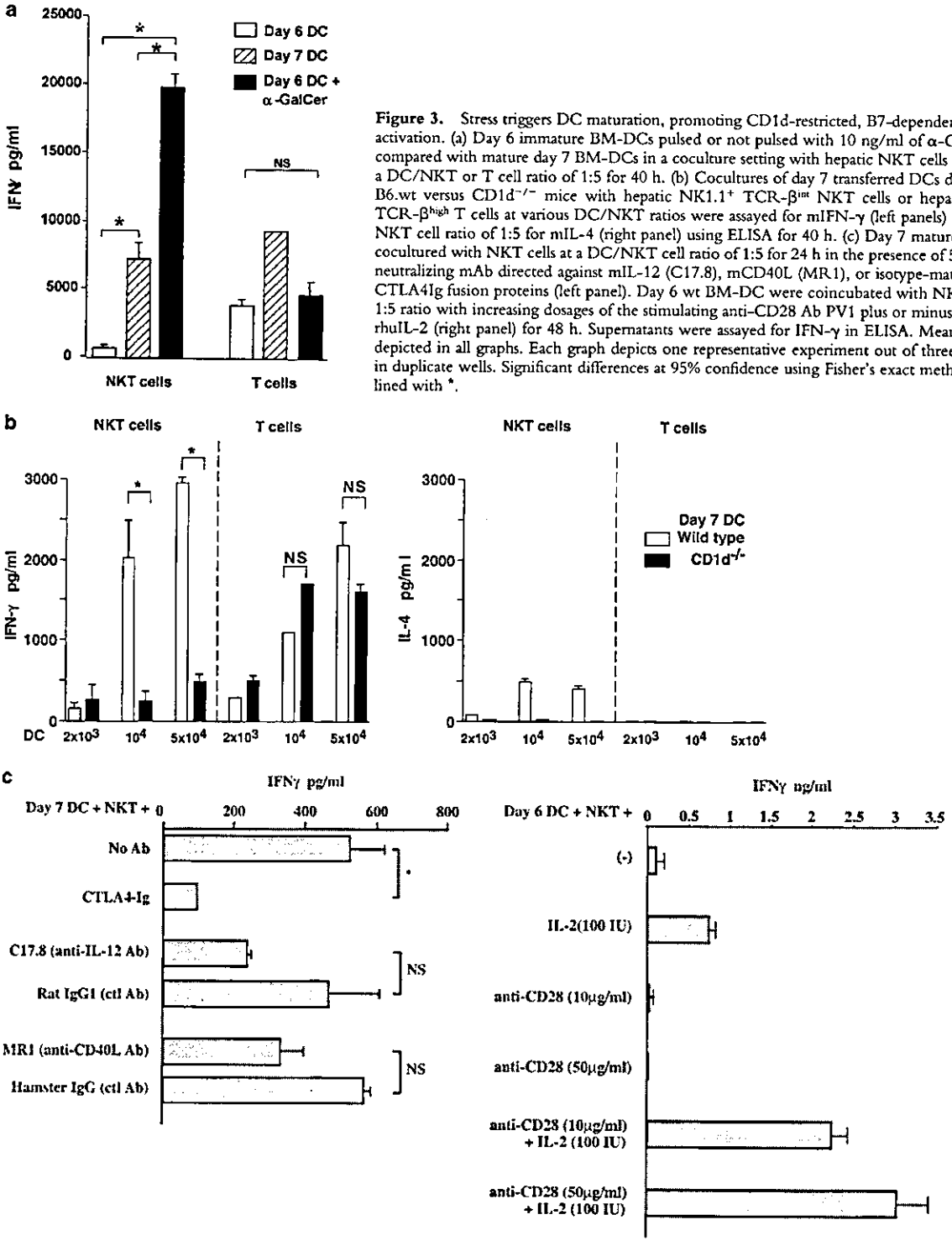

Figure 3. Stress triggers DC maturation, promoting CD1d-restricted, B7-dependent NKT cell activation. (a) Day 6 immature BM-DCs pulsed or not pulsed with 10 ng/ml of α-GalCer were compared with mature day 7 BM-DCs in a coculture setting with hepatic NKT cells or T cells at a DC/NKT or T cell ratio of 1:5 for 40 h. (b) Cocultures of day 7 transferred DCs derived from B6.wt versus CD1d$^{-/-}$ mice with hepatic NK1.1^{+} TCR-β^{int} NKT cells or hepatic NK1.1^{-} TCR-β^{high} T cells at various DC/NKT ratios were assayed for mIFN-γ (left panels) and at DC/NKT cell ratio of 1:5 for mIL-4 (right panel) using ELISA for 40 h. (c) Day 7 mature DCs were cocultured with NKT cells at a DC/NKT cell ratio of 1:5 for 24 h in the presence of 50 μg/ml of neutralizing mAb directed against mIL-12 (C17.8), mCD40L (MR1), or isotype-matched Ab or CTLA4Ig fusion proteins (left panel). Day 6 wt BM-DC were coincubated with NKT cells at a 1:5 ratio with increasing dosages of the stimulating anti-CD28 Ab PV1 plus or minus 100 IU/ml rhuIL-2 (right panel) for 48 h. Supernatants were assayed for IFN-γ in ELISA. Means ± SE are depicted in all graphs. Each graph depicts one representative experiment out of three performed in duplicate wells. Significant differences at 95% confidence using Fisher's exact method are outlined with *.

(AMVPKTLLL) that does not bind Qa-1) at increasing dosages on H-2D$^{b/-}$ BM-DC, (b) or using the neutralizing mAb anti–H-2D^{b} or anti–H-2K^{b} pulsed onto wt day 6 BM-DCs before NKT cell coculture. Only 20–25% of hepatic NKT cells (TCRβ^{int}/NK1.1^{+}) express CD94 molecules (among which not all coexpress NKG2A molecules) i.e. up to 4% of bulk liver mononuclear cells (not shown). The amounts of IFN-γ secreted from NKT cells in cocul-

ture with day 6 immature wt versus H-2D$^{b-/-}$ BM-DCs incubated with increasing dosages of Qa-1^b binding peptides were compared (1–30 μM of Qdm1 or R5K mock peptides). No significant inhibition of IFN-γ production was observed using Qdm1 peptides pulsed onto H-2D$^{b-/-}$ BM-DCs (not shown). In accordance with this result, the neutralizing anti–Qa-1^b mAb did not allow IFN-γ production by NKT cells cocultured with wt day 6 BM-DCs (not shown). The right panel of Fig. 2 c investigates the direct inhibitory pathway and compares the secretion levels of IFN-γ by NKT cells stimulated by wt day 6 BM-DCs incubated with 10 to 50 μg/ml of neutralizing anti–H-2D$^{b-/-}$ or anti–H-2K$^{b-/-}$ Ab. Significant IFN-γ secretion is found only using the anti–H-2D$^{b-/-}$ Ab, although nanogram levels were achieved using mature DCs (not shown on this graph). Therefore, in line with the well known heterogeneity of the NKT cell population, a complex inhibitory pathway likely participates in maintaining DC-mediated tolerance of liver resident NKT cells.

These data imply that H-2 class Ia and Ib molecules differentially and constitutively prevent DC-mediated IFN-γ production from resting liver NKT cells and that CD1d-restricted antigens are presented electively by DC to NKT cells in vitro.

Stressed DCs Become Capable of Stimulating NKT Cells. However, in stress conditions shown to be mimicked by cell harvest and transfer into new plastic dishes (29) or by LPS, wt DCs became activated and acquired a more mature phenotype i.e. MHC class II^{bright}, CD80$^+$, CD86$^+$, and CD40$^+$ ("transferred" day 7 DCs, Fig. 1) displaying potent allostimulatory capacity (not shown) while CD1d was not significantly overexpressed (Fig. 1). Moreover, the expression levels of the H-2K and H-2D molecules were comparable at day 7 (Fig. 1). After their transfer at day 6, day 7 wt DCs acquired the capacity to foster NKT cells toward a Th1 predominant secretion pattern while pulsing with KRN7000 in such conditions led to secretion of both IL-4 and IFN-γ at high levels (not shown). High levels of IFN-γ were measured in 22–40 h coculture supernatants (Fig. 3 a) while IL-4 was barely detectable (Fig. 3 b). Mature DCs stimulated NKT cells in a dose-dependent manner (Fig. 3 b), with optimal effects at a ratio of 1 DC:1 NKT cell (Fig. 3 b). Similar NKT cell activation was obtained using LPS-activated DCs (not shown). No significant thymidine incorporation by NKT cells was measured in proliferation assays and trypan blue exclusion did not show increased numbers of viable NKT cells after 40 h incubation with mature DCs (not shown). The mature DC/NKT cell cross-talk was significantly inhibited when DCs were generated from B6.CD1d$^{-/-}$ mice (Fig. 3 b). Inhibition was also clear for IL-4 secretion (Fig. 3 b). The phenotype of mature DCs in B6 wt and B6.CD1d$^{-/-}$ mice was comparable (not shown). Eberl et al. (30) pointed out a tissue-specific segregation of CD1d-dependent and -independent NKT cells, hepatic NKT cells being mostly CD1d dependent. In similar conditions of B6 liver cell sorting, CD3$^+$/NK1.1$^-$ hepatic T cells also produce, albeit less efficiently, detectable amounts of IFN-γ (but no IL-4) when placed in close contact with mature DCs. It is noteworthy that, in contrast to NKT cell activation, T cell activation was not regulated by CD1d molecules nor α-GalCer (Fig. 3 b). It is unlikely that IFN-γ is secreted from DCs rather than NKT cells in these cocultures as only CD8$^+$ DCs were shown to produce IFN-γ after stimulation with ng levels of both IL-12 and IL-18 (31).

The DC maturation allowed to overcome H-2 class Ia–mediated constitutive NKT cell inhibition by DCs, as comparable levels of IFN-γ were secreted by NKT cells in contact with wt versus K$^{b-/-}$D$^{b-/-}$ mature DCs (data not shown). However, the synthetic α-GalCer–mediated

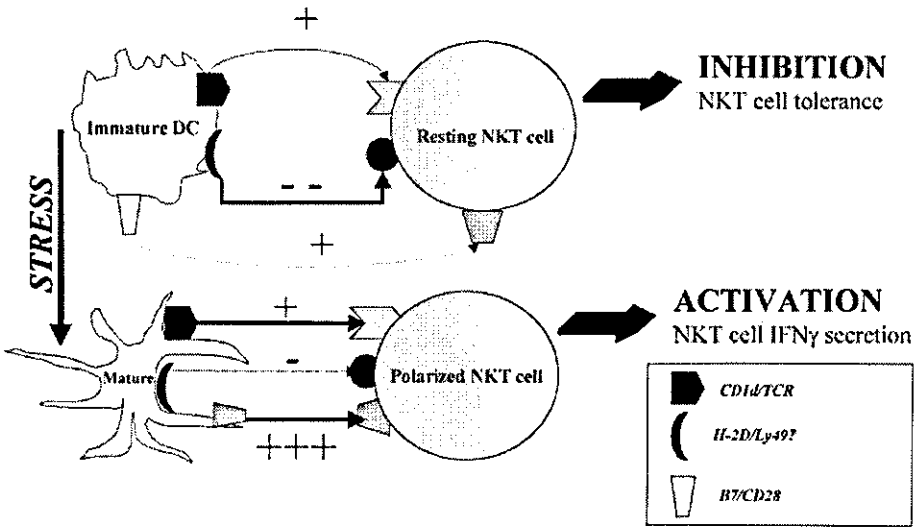

Figure 4. Putative schematic representation of the DC/NKT cell cross-talk. Tissue resident DCs (immature stage) constitutively inhibit CD1d-dependent NKT cell IFN-γ production (first signal: CD1d/TCR) through a mechanism involving H-2 class I molecules (second signal: H-2D/Ly49? +/− CD94/NKG2A ?). The inhibitory pathway might be dominant because a third accessory pathway overruling the dominant negative signal is lacking on immature DCs. In contrast, after stress (LPS, transfer), DCs acquire a third accessory signal (B7/CD28) that is dominant over the second inhibitory pathway allowing CD1d-restricted DC antigen presentation. It is conceivable that in pathological conditions where high IFN-γ levels are required, DCs become capable of triggering NKT cell recognition of self and/or foreign antigens presented by MHC class Ib molecules to the canonical TCR.

CD1d stimulation was more potent, even at low dosage (1–10 ng/ml) than the self DC antigens and Th0 biased. The low levels of CD1d-dependent IL-4 secretion by NKT cells triggered by mature DCs could be accounted for by the relative weakness of the CD1d-mediated presentation of DC self-antigens (Fig. 3, a and b) and/or discrete threshold of reactivity of various hepatic NKT cell subsets.

The B7/CD28 Pathway Overrides the H-2D^b-mediated NKT Cell Inhibition. We next investigated the mechanisms accounting for NKT cell IFN-γ secretion after contact with stressed DCs. During α-GalCer–mediated NKT cell stimulation, IL-12 and CD40 were shown to play a critical role (3, 12). However, despite the Th1 predominant pattern, IL-12 p70 was not detectable in ELISA in NKT cell cocultures with mature DCs where significant IFN-γ levels were measured (not shown). However, as neutralizing anti–IL-12 mAb decreased IFN-γ secretion, albeit not significantly (mostly at early time points 24 h of the coculture), it remains conceivable that IL-12 be involved after the initial CD1d/TCR interaction step (Fig. 3 c, left panel). Moreover, in transwell experiments whereby mature DCs and NKT cells are physically separated by a porous membrane, IFN-γ was not produced suggesting a dominant role for a membrane-associated molecule in the DC/NKT cell cross-talk (data not shown). Therefore, we next investigated whether costimulatory molecules upregulated upon maturation could account for circumvention of H-2 class I–mediated inhibition. Saturating concentrations of neutralizing mAb directed against CD40L or B7 molecules were used in the DC/NKT cell cocultures. While a partial but not significant inhibition was observed using neutralizing anti-CD40L mAb, CTLA4Ig fusion proteins were shown to be necessary and sufficient to completely abrogate the DC/NKT cell cross-talk in vitro. Both, NKT cell IFN-γ (Fig. 3 c, left panel) and IL-4 secretion (not shown) were suppressed. To confirm that CD28 engagement is sufficient to trigger hepatic NKT cell IFN-γ production by DCs, wt BM-DCs at day 6 (immature cells) were cocultured with hepatic NKT cells in the presence of stimulating anti-CD28 mAb (PV.1) with or without low doses of IL-2 (100 IU/ml). H-2 class I–mediated inhibition could be efficiently overcome using the anti-CD28 mAb plus IL-2 with a synergistic effects between the cytokine and the costimulatory factor (Fig. 3 c, right panel). The IFN-γ levels were fairly comparable with those achieved using mature BM-DCs (day7). Altogether, the B7/CD28 pathway is critical to account for the ability of activated DCs to trigger NKT cell IFN-γ production by circumventing class I inhibition.

A Schematic View of the DC/NKT Cell Cross-Talk In Vitro. These data demonstrate that stress-induced DC activation allows to overcome constitutive inhibitory pathways through B7/CD28 interaction, thereby promoting CD1d-dependent IFN-γ production by NKT cells in vitro (Fig. 4). The role of CD1d and B7 expression levels, of DC endogenous antigens and/or tissue origin need to be investigated to ascribe these regulatory NKT activation pathways to BM-DCs. We showed that DCs and not adherent splenocytes (antigen-presenting cells expressing high levels of CD1d molecules, and low levels of I-A^b, B7.2 molecules), when devoid of inhibitory receptor ligand, trigger NKT cell activation. Such a difference may be accounted for by tissue origin. Indeed, while activated BM-DCs could trigger IFN-γ production, Flt3L splenic DCs after overnight activation were not able to activate NKT cells (not shown). It is also possible that B7.1 is critical to overcome H-2 class I–mediated inhibition because adherent splenocytes do not express B7.1. Intracellular trafficking of CD1d molecules may play a critical role in determining the antigens presented by DCs.

It is noteworthy that DC-mediated NKT cell activation is leading predominantly to Th1 secretion pattern in vitro, suggesting that this regulatory pathway may be relevant in the setting of intracellular pathogens, viruses, or tumors. IFN-γ is a pleiotropic cytokine playing a central role in promoting innate and adaptive mechanisms of host defense. IFN-γ not only fosters T cell–mediated immunity but also activates macrophages, promotes antigen processing, and presentation by antigen-presenting cell and prevents viral replication, angiogenesis, and transformed cell growth (32). Therefore, it is conceivable that dysregulation of DC functions suggested in autoimmune disorders or tumors might foster NKT cell reactivity toward inappropriate Th pattern. Further investigations will be required to unravel the in vivo dynamics between DCs and NKT cells during infection, autoimmunity, or tumor development but such data outline that CD1d-restricted DC antigens might be relevant in such disorders.

We thank KIRIN Brewery Company Ltd. (Tokyo, Japan) for providing KRN7000 to the National Cancer Center. We are indebted to the animal facility staff of IGR and to Valérie Schiavon for technical assistance. We are grateful to Nadine Fernandez and D. Raulet for helpful discussion and advice.

Y. Ikarashi was supported by the research fellowship program of collaborative works for Japanese researchers in foreign institutes, i.e., the Japanese Foundation for Promotion of Cancer Research supported by the Ministry of Health and Welfare for the second Term Comprehensive 10-yr strategy for cancer control. R. Mikami was supported by the Ministry of Foreign Affairs. The work was also supported by the french fellowship GEFLUC, LIGUE française contre le cancer, and Association de la Recherche le Cancer (ARC).

Submitted: 3 January 2001
Revised: 9 August 2001
Accepted: 21 August 2001

References

1. Bendelac, A., M.N. Riversa, S.H. Park, and J.H. Roark. 1997. Mouse CD1-specific NK1$^+$ T cells: development, specificity, and function. *Annu. Rev. Immunol.* 15:535–562.
2. MacDonald, H.R. 1995. NK1.1$^+$ T cell receptor α/β cells: new clues to their origin, specificity and function. *J. Exp. Med.* 182:633–638.
3. Kawano, T., J. Cui, Y. Koezuka, I. Toura, Y. Kaneko, K. Motoki, H. Ueno, R. Nakagawa, H. Sato, E. Kondo, et al. 1997. CD1d-restricted and TCR-mediated activation of Vα14 NKT cells by glycosylceramides. *Science.* 278:1626–

1629.
4. Spada, F.M., Y. Koezuka, and S.A. Porcelli. 1998. CD1d-restricted recognition of synthetic glycolipid antigen by human natural killer T cell. *J. Exp. Med.* 188:1529–1534.
5. Burdin, N., L. Brossay, Y. Koezuka, S.T. Smily, M. Gurusby, M. Gui, M. Taniguchi, K. Hayakawa, and M. Kronenberg. 1998. Selective ability of mouse CD1 to present glycolipids. α-galactosylceramide specifically stimulates Vα14 NKT lymphocytes. *J. Immunol.* 161:3271–3281.
6. Cui, J., T. Shin, T. Kawano, H. Sato, E. Kondo, I. Toura, Y. Kaneko, H. Koseki, M. Kanno, and M. Taniguchi. 1997. Requirement for Vα14 NKT cells in IL-12-mediated rejection of tumor. *Science.* 278:1623–1626.
7. Kawano, T., J. Cui, Y. Koezuka, I. Toura, Y. Kaneko, H. Sato, E. Kondo, M. Harada, H. Koseki, T. Nakayama, et al. 1998. Natural killer-like nonspecific tumor lysis mediated by specific ligand-activated Vα14 NKT cells. *Proc. Natl. Acad. Sci. USA.* 95:5690–5693.
8. Smyth, M.J., K.Y.T. Thia, S.E.A. Street, E. Cretney, J.A. Trapani, M. Taniguchi, T. Kawano, S.B. Pelikan, N.Y. Crowe, and D.I. Godfrey. 2000. Differential tumor surveillance by natural killer (NK) and NKT cells. *J. Exp. Med.* 191: 661–668.
9. Smyth, M.J., M. Taniguchi, and S.E. Street. 2000. The anti-tumor activity of IL-12: mechanisms of innate immunity that are model and dose-dependent. *J. Immunol.* 165:2265–2670.
10. Nakagawa, R., K. Motoki, H. Nakamura, H. Ueno, R. Iijima, A. Yamaguchi, S. Tsuyuki, T. Inamoto, and Y. Koezuka. 1998. Antitumor activity of α-galactosylceramide, KRN7000, in mice with EL-4 hepatic metastasis and its cytokine production. *Oncol. Res.* 10:561–568.
11. Wilson, S.B., S.C. Kent, K.T. Patton, T. Orban, R.A. Jackson, M. Exely, S. Porcelli, D. Schatz, M.A. Atkinson, S.P. Balk, et al. 1998. Extreme Th1 bias of invariant Vα24JaQT cells in type 1 diabetes. *Nature.* 391:177–181.
12. Kitamura, H., K. Iwakabe, T. Yahata, S. Nishimura, A. Ohta, Y. Ohmi, M. Sato, K. Takeda, K. Okumura, L. Van Kaer, et al. 1999. The natural killer T (NKT) cell ligand α-galactosylceramide demonstrates its immunopotentiating effect by inducing interleukin (IL)-12 producing by dendritic cell and IL-12 receptor expression on NKT cells. *J. Exp. Med.* 189:1121–1127.
13. Burdin, N., L. Brossay, and M. Kronenberg. 1999. Immunization with α−galactosylceramide polarizes CD1d-reactive NK T cells towards Th2 cytokine synthesis. *Eur. J. Immunol.* 29:2014–2025.
14. Yoshimoto, T., A. Bendelac, C. Watson, J. Hu-Li, and W.E. Paul. 1995. Role of NK1.1+ T cells in a Th2 response and in IgE production. *Science.* 270:1845–1847.
15. Terabe, M., S. Matsui, N. Noben-Trauth, H. Chen, C. Watson, D.D. Donaldson, D.P. Carbone, W.E. Paul, and J.A. Berzofsky. NKT cell-immunosurveillance by IL-13 and the IL-4R-STAT6 pathway. *Nat. Immunol.* 1:515–520.
16. Gumperz, J.E., C. Roy, A. Makowaska, D. Lum, M. Sugita, T. Podrebarac, Y. Koezuka, S.A. Porcelli, S. Cardell, M.B. Brenner, and S.M. Behar. 2000. Murine CD1d-restricted T cell recognition of cellular lipids. *Immunity.* 12:211–221.
17. Brossay, L., S. Tangri, M. Bix, S. Cardell, R. Locksley, and M. Kornenberg. 1997. Mouse CD1-autoreactive T cells have diverse patterns of reactivity to $CD1^+$ targets. *J. Immunol.* 160:3681–3688.
18. Park, S.H., J.H. Roark, and A. Bendelac. 1998. Tissue-specific recognition of mouse CD1 molecules. *J. Immunol.* 160: 3128–3134.
19. Chiu, Y.H., J. Jayawardena, A. Weiss, D. Lee, S.H. Park, V. Dautry-Varsat, and A. Bendelac. 1999. Distinct subset of CD1d-restricted T cells recognize self-antigen loaded in different cellular compartments. *J. Exp. Med.* 189:103–110.
20. Fernandez, N.C., A. Lozier, C. Flament, P. Ricciardi-Castagnoli, D. Bellet, M. Suter, M. Perricaudet, T. Tursz, E. Maraskovsky, and L. Zitvogel. 1999. Dendritic cells directly trigger NK cell function: cross-talk relevant in innate anti-tumor immune responses in vivo. *Nat. Med.* 5:405–411.
21. Vugmeyster, Y., R. Glas, B. Pérarnau, F.A. Lemonnier, H. Eisen, and H. Ploegh. 1998. Major histocompatibility complex (MHC) class I $K^bD^{b-/-}$ deficient mice possess functional $CD8^+$ T cells and natural killer cells. *Proc. Natl. Acad. Sci. USA.* 95:1249–12497.
22. Park, S.H., D. Guy-Grand, F.A. Lemonnier, C.R. Wang, A. Bendelac, and B. Jabri. 1999. Selection and expansion of $CD8\alpha/\alpha^+$ T cell receptor α/β^+ intestinal intraepithelial lymphocytes in the absence of both classical major histocompatibility complex class I and non classical CD1 molecules. *J. Exp. Med.* 190:885–890.
23. Shinohara, K., Y. Ikarashi, H. Maruoka, M. Miyata, T. Sugimura, M. Terada, and H. Wakasugi. 1999. Functional and phenotypical characteristics of hepatic NK-like T cells in NK1.1+ and − mouse strains. *Eur. J. Immunol.* 29:1871–1878.
24. Azuma, M., K. Kato, Y. Ikarashi, R. Asada-Mikami, H. Maruoka, Y. Takaue, A. Saito, and H. Wakasugi. 2000. Cytokines production of U5A2-13-positive T cells by stimulation with glycolipid α-galactosylceramide. *Eur. J. Immunol.* 30:2138–2146.
25. MacDonald, H.R., K. Rosemary, K. Lees, and W. Held. 1998. Developmentally regulated extinction of Ly-49 receptor expression permits maturation and selection of $NK1.1^+$ T cells. *J. Exp. Med.* 187:2109–2114.
26. Skold, M., and S. Cardell. 2000. Differential regulation of Ly49 expression on $CD4^+$ and $CD4^-CD8^-$ (double negative) $NK1.1^+$ T cells. *Eur. J. Immunol.* 30:2488–2496.
27. Vance, R.E., J.R. Kraft, J.D. Altman, P.E. Jensen, and D.H. Raulet. 1998. Mouse CD94/NKG2A is a natural killer cell receptor for the nonclassical MHC class I molecule $Qa\text{-}1^b$. *J. Exp. Med.* 188:1841–1848.
28. Kraft, J.R., R.E. Vance, J. Phol, A.M. Martinet. D.H. Raulet, and P.E. Jensen. 2000. Analysis of Qa-1(b) peptide binding specificity and capacity of CD94/NKG2A to discriminate between Qa-1-peptide complexes. *J. Exp. Med.* 192:613–624.
29. Gallucci, S., M. Lolkema, and P. Matzinger. 1999. Natural adjuvants: endogenous activators of dendritic cells. *Nat. Med.* 5:1249–1255.
30. Eberl, G., R. Lees, S.T. Smily, M. Taniguchi, M.J. Grusby, and H.R. MacDonald. 1999. Tissue-specific segregation of CD1d-dependent and CD1d independent NKT cells. *J. Immunol.* 162:6410–6419.
31. Ohteki, T., T. Fukao, K. Suzue, C. Maki, M. Ito, M. Nakamura, and S. Koyasu. 1999. Interleukin 12-dependent interferon γ production by $CD8\alpha^+$ lymphoid dendritic cells. *J. Exp. Med.* 189:1981–1986.
32. Kaplan, D.H., V. Shankaran, A.S. Dighe, E. Stockert, M. Aguet, L.J. Old, and R.D. Schreiber. 1998. Demonstration of an interferon γ−dependent tumor surveillance system in immunocompetent mice. *Proc. Natl. Acad. Sci. USA.* 95: 7556–7561.

THE JOURNAL OF BIOLOGICAL CHEMISTRY
Vol. 278, No. 47, Issue of November 21, pp. 47217–47222, 2003
Printed in U.S.A.

Multimerization of the Receptor Activator of Nuclear Factor-κB Ligand (RANKL) Isoforms and Regulation of Osteoclastogenesis*

Received for publication, May 2, 2003, and in revised form, September 16, 2003
Published, JBC Papers in Press, September 17, 2003, DOI 10.1074/jbc.M304636200

Tohru Ikeda‡§, Michiyuki Kasai¶, Junko Suzuki‡‖, Hiroyuki Kuroyama‡, Sachiko Seki‡, Masanori Utsuyama‡, and Katsuiku Hirokawa‡

From the Departments of ‡Pathology and Immunology and ‖Geriatric Dentistry, Graduate School, Tokyo Medical and Dental University, 1-5-45 Yushima, Bunkyo-ku, Tokyo 113-8519 and the ¶Department of Safety Research on Blood and Biological Products, National Institute of Infectious Diseases, Toyama, 1-23-1 Shinjuku-ku, Tokyo 162-8640, Japan

The receptor activator of nuclear factor-κB ligand (RANKL), a member of the tumor necrosis factor family, is a transmembrane protein, which is known as an essential initiation factor of osteoclastogenesis. Previously, we identified three RANKL isoforms. RANKL1 was identical to the originally reported RANKL. RANKL2 had a shorter intracellular domain. RANKL3 did not have the intracellular or transmembrane domains and was suggested to act as a soluble form protein. Here, we show that RANKL forms homo- or heteromultimers. NIH3T3 cells transfected with RANKL1 or RANKL2 form mononuclear tartrate-resistant acid phosphatase-positive preosteoclasts in an *in vitro* osteoclastogenesis assay system. Coexpression of RANKL1 and RANKL2 induces multinucleated osteoclasts. RANKL3 has no effect on the formation of preosteoclasts or osteoclasts but significantly inhibits fusion of preosteoclasts when coexpressed with RANKL1 and RANKL2. These findings imply the presence of multiple multimeric structures of RANKL, which may regulate bone metabolism.

The receptor activator of nuclear factor-κB ligand (RANKL[1] also known as OPGL, ODF, or TRANCE) is a type II TNF-like transmembrane protein, which plays fundamental roles for fusion of preosteoclasts by binding to the receptor, receptor activator of nuclear factor-κB (RANK) (1, 2). Another soluble form receptor-like molecule, osteoprotegerin (OPG), binds to RANKL and inhibits osteoclastogenesis by competitive inhibition of the signaling through the RANKL/RANK system (3, 4). Osteoclastogenesis is efficiently reproduced by an *in vitro* coculture system using macrophages and bone marrow stromal cells (5, 6). In the presence of recombinant RANKL protein, osteoclasts were formed without bone marrow stromal cells (7–9). The essential role of the RANKL/RANK system in osteoclastogenesis was confirmed in mice with a disrupted *RANKL* gene and mice with disruption of the *RANK* gene, both of which showed severe osteopetrosis (10–12).

Previously, we identified three RANKL isoforms from mouse cDNA and named them RANKL1, RANKL2, and RANKL3 (13). RANKL1 was identical to the originally reported RANKL. RANKL2 had a shorter intracellular domain. RANKL3 did not have the intracellular or transmembrane domains and was suggested to be a soluble form protein. Previous findings showed that both tumor necrosis factor (TNF)-α and TNF-β formed trimers, and the multimeric structure was essential for expressing the activities of the molecules (14–16). These findings strongly suggest that another member of this family, RANKL, also forms a multimeric structure. Recently, the crystal structure of the extracellular domain of mouse RANKL was determined, and it was shown to form a trimeric structure (17, 18). The present study revealed that the mouse RANKL isoforms interact and express different biological activities.

EXPERIMENTAL PROCEDURES

Transfection and Selection—For immunoprecipitation and confocal microscopy, the protein-coding region of cDNA for each RANKL isoform was cloned into pEGFP-N2 and pDsRed-N1 vectors (Clontech), both of which express the product of inserted cDNA as a fusion to the N terminus of fluorescent protein, EGFP and DsRed, respectively. For osteoclastogenesis assay, each RANKL isoform was cloned into selectable mammalian expression vector, pMIK HygB (13), pcDNA3.1 (Invitrogen), or pEFBOSbsr (19). Transfections were performed using the TransFast transfection reagent (Promega). NIH3T3 cells transfected with pMIK HygB-RANKL were cultured in α-minimal essential medium with 10% fetal bovine serum and 250 μg/ml Hygromycin B (Calbiochem). In some clones expressing each RANKL isoform, pcDNA3.1-RANKL was additionally transfected. The cells were selected and maintained in the medium supplemented with 500 μg/ml Geneticin (Sigma) in addition to the Hygromycin B. To obtain cells expressing RANKL1, RANKL2, and RANKL3, pEFBOSbsr-RANKL3 was further transfected to the cells expressing RANKL1 and RANKL2. Cells were selected and maintained in the medium supplemented with 0.2 μg/ml Blasticidin S hydrochloride (Funakoshi) in addition to the Hygromycin B and Geneticin. The expression of each RANKL isoform was analyzed by reverse transcriptase (RT)-PCR and Northern hybridization. RT-PCR was performed as described previously (13) using forward primers, 5′-CTGAGCTATTCCAGAAGTAGTGAGGAGG-3′, 5′-CTGCAGATATCCAGCACAGTGGCG-3′, and 5′-TCGCAACGGGTTTGCCGCCAGAAC-3′, which recognized downstream from the transcriptional initiation site of pMIK HygB, pcDNA3.1, and pEFBOSbsr, respectively, and a common reverse primer, 5′-TCAGTCTATGTCCTGAACTTTGAAAGCCCC-3′, which recognized the 3′ end of the inserted mouse RANKL cDNA. Northern hybridization was performed as described previously (13).

Immunoprecipitation—RANKL-pDsRed and/or RANKL-pEGFP were transfected to NIH3T3 cells plated in 100-mm-type culture dishes. After 48 h, cells were collected and lysed with 1 ml of lysis buffer (Tris-buffered saline (pH 7.1) containing 1% digitonin, 1 mM EDTA, 0.02% NaN_3, 1 mM phenylmethanesulfonyl fluoride, 100 μM *N-p*-tosyl-

* This work was supported by Grant-in-aid for Scientific Research 15591963 from the Japan Society for the Promotion of Science. The costs of publication of this article were defrayed in part by the payment of page charges. This article must therefore be hereby marked "*advertisement*" in accordance with 18 U.S.C. Section 1734 solely to indicate this fact.

§ To whom correspondence should be addressed. Tel.: 81-3-5803-5176; Fax: 81-3-5803-0123; E-mail: toru.pth2@med.tmd.ac.jp.

[1] The abbreviations used are: RANKL, RANK legand; RANK, receptor activator of nuclear factor-κB; OPG, osteoprotegerin; OPGL, OPG ligand; ODF, osteoclast differentiation factor; TRANCE, tumor necrosis factor-related activation induced cytokine; TNF, tumor necrosis factor; RT, reverse transcriptase; EGS, ethylene glycol bis(succinimidylsuccinate); TRAP, tartrare-resistant acid phosphatase; CT-R, calcitonin receptor; GFP, green fluorescent protein; EGFP, enhanced GFP; DsRed, red fluorescent protein.

L-phenylalanine chloromethyl ketone, 10 μM leupeptin, and 10 μg/ml aprotinin), and the supernatants were precleared with Sepharose 4B coupling with 100 μg of rabbit immunoglobulins and incubated with 40 μg of rabbit anti-DsRed-peptide antibody (Clontech, catalog number 8370) cross-linked to immobilized Protein G (Pierce, catalog number 45210) for 72 h. The immune complexes were washed with lysis buffer three times and eluted with 100 μl of elution buffer (1% digitonin, 50 mM glycin-HCl (pH 3.0), 150 mM NaCl, 0.02% NaN_3). The eluant was adjusted to pH 7.0 with 1 M Tris-HCl (pH 9.0). Samples were separated by 10% SDS-PAGE and transferred electrophoretically onto nitrocellulose membranes (Schleicher & Schuell). Immunoblotting was performed using the rabbit anti-DsRed-peptide antibody or a mouse anti-GFP monoclonal antibody (Clontech, catalog number 8371). Immunoreactive proteins were visualized using the ECL Western blotting detection kit (Amersham Pharmacia Biotech).

Cross-linking of Recombinant RANKL3 Protein—Five μg of recombinant mouse RANKL3 (13) was treated with 1.2 mg/ml ethylene glycol bis(succinimidylsuccinate) (EGS) (Pierce) at 4 °C for 2 h. Part of the cross-linked samples was cleaved using 1 M hydroxylamine hydrochloride (Pierce), pH 8.5, at 37 °C for 4 h. The samples were separated by 10% SDS-PAGE and visualized by Coomassie Brilliant Blue staining.

Confocal Microscopy—RANKL-pDsRed and/or RANKL-pEGFP were transfected to NIH3T3 cells plated on 35-mm glass-bottom dishes (Iwaki Glass). After 48 h, they were viewed before or after fixation with 3.8% formaldehyde in phosphate-buffered saline using an LSM 510 laser scanning confocal microscope (Zeiss) equipped with a ×63 water immersion objective. EGFP was examined using the 488-nm line of the argon-krypton laser and a set of the 488-nm main splitter and the 505–530-nm band pass emission. DsRed was examined using the 543-nm line of the helium-neon laser and a set of the 488/543-nm main splitter HFT and the 560-nm long pass emission.

Osteoclastogenesis Assays and Cytochemical Staining—Mouse bone marrow macrophages were prepared from femora and tibiae of 5-week-old female ddy mice as described previously (20, 21). Using 48-well plates, the bone marrow macrophages (1.5×10^5 cells/well) were cocultured with NIH3T3 cells expressing RANKL isoform(s) (1.5×10^4 cells/well) in 0.25 ml/well of α-minimal essential medium supplemented with 10% fetal bovine serum, 30 ng/ml macrophage colony-stimulating factor, 1×10^{-8} M of 1α,25-dihydroxyvitamin D_3, and 1×10^{-7} M of dexamethasone. After 5–10 days of culture, cells were fixed with 4% formaldehyde in phosphate-buffered saline (−) for 10 min and ice-cold methanol-acetone (1:1) for 2 min. Tartrate-resistant acid phosphatase (TRAP) was stained with 0.1 M sodium acetate buffer (pH 5.0) containing 0.1 mg/ml naphthol AS-MX phosphate (Sigma), 0.6 mg/ml fast red AL salt (Sigma), and 50 mM sodium tartrate (Wako). Statistical significance was evaluated using the Mann-Whitney *U* test. Animal care was in accordance with guidelines for animal welfare in Tokyo Medical and Dental University.

In Vitro Formation of Resorption Lacunae—Whale dentin slices were placed on 48-well plates, and cocultures were performed on them (5). Ten days after the culture period, the slices were soaked in 4 M guanidine thiocyanate solution for 24 h, rinsed with distilled water, and stained with Meyer's hematoxylin. The area of resorption lacunae was quantified using the net micrometer disk in the eyepiece of a microscope, and the ratios of standard areas with resorption lacunae to the areas with and without resorption lacunae were calculated (22). The statistical significance was evaluated using the Mann-Whitney *U* test.

Immunohistochemistry—Cells were treated with 0.1% hydrogen peroxide in 95% methanol for 5 min, rinsed with phosphate-buffered saline, and treated with 2% bovine serum albumin (Serologicals Proteins) at 4 °C overnight. An antibody against calcitonin receptors (CT-Rs) (Santa Cruz Biotechnology, catalog number 8860) or the antibody preabsorbed with the blocking peptide (Santa Cruz Biotechnology) was applied on the specimens and incubated at 4 °C overnight. After rinsing with phosphate-buffered saline, immunohistochemistry was performed using the ENVISION Plus system (DAKO).

RESULTS

Interaction of Three RANKL Isoforms—Constructs of RANKL1, RANKL2, and RANKL3 with a tag of EGFP at the C terminus and RANKL1, RANKL2, and RANKL3 with a tag of DsRed at the C terminus were transfected to NIH3T3 cells and served for immunoprecipitation and Western blotting. The expression of transfected RANKL1-DsRed (Fig. 1*A*, *lanes 1–4*) and RANKL2-DsRed (Fig. 1*A*, *lane 5*) was detected in whole cell lysates with the anti-DsRed antibody (Fig. 1*A*). The expression of RANKL1-EGFP (Fig. 1*B*, *lane 2*), RANKL2-EGFP (Fig. 1*B*, *lane 3*), and RANKL3-EGFP (Fig. 1*B*, *lanes 4* and *5*) was detected with the anti-EGFP antibody. Immunoprecipitation of RANKL-DsRed with the anti-DsRed antibody was confirmed using the same antibody. Immunoprecipitation of RANKL1-DsRed (Fig. 1*C*, *lanes 1–4*) and RANKL2-DsRed (Fig. 1*C*, *lane 5*) was detected among nonspecific background signals. In the specimens cotransfected with RANKL1-DsRed and RANKL1-EGFP and immunoprecipitated with the anti-DsRed antibody, coprecipitation of RANKL1-EGFP protein was detected with the anti-EGFP antibody (Fig. 1*D*, *lane 2*). Coprecipitation of RANKL2-EGFP was also detected in the specimen cotransfected with RANKL1-DsRed and RANKL2-EGFP (Fig. 1*D*, *lane 3*). In the specimens cotransfected with RANKL1-DsRed and RANKL3-EGFP in addition to RANKL2-DsRed and RANKL3-EGFP, no RANKL3-EGFP protein was detected (Fig. 1*D*, *lanes 4* and *5*).

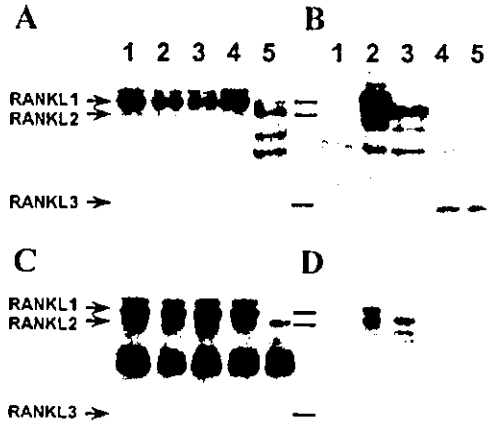

FIG. 1. **Interactions between RANKL isoforms.** NIH3T3 cells transfected with the cDNA encoding DsRed-tagged RANKL1 (*lane 1*), DsRed-tagged RANKL1 and EGFP-tagged RANKL isoforms (*lane 2*; RANKL1, *lane 3*; RANKL2, and *lane 4*; RANKL3, respectively), and DsRed-tagged RANKL2 and EGFP-tagged RANKL3 (*lane 5*) are shown. *A* and *B*, Western blotting of whole cell lysates. *C* and *D*, Western blotting of RANKL isoforms immunoprecipitated with the rabbit anti-DsRed antibody. Membranes were probed using the anti-DsRed antibody (*A* and *C*) or the anti-EGFP antibody (*B* and *D*), respectively.

To confirm the interaction of RANKL3 protein, recombinant RANKL3 protein was cross-linked with EGS and visualized by Coomassie Brilliant Blue staining. Recombinant RANKL3 treated with EGS revealed a trimer (66 kDa) and a small amount of dimer (44 kDa) (Fig. 2, *lane 2*), which was specifically cleaved by hydroxylamine hydrochloride to a dimer and monomer (Fig. 2, *lane 3*). Similar results were also obtained using bis-[2-(succinimidooxycarbonyloxy)ethyl]sulfone (BSOCOES) as the cross-linker.[2]

In addition, intracellular localization of three RANKL isoforms was analyzed by means of detecting the tagged fluorescence protein using a confocal microscope. Both RANKL1 and RANKL2 were scattered as rough dots over the cytoplasmic region of the cells, but RANKL3 was located as fine granules over the cells (Fig. 3, *A–C*). In the cells cotransfected with RANKL1-DsRed and RANKL1-EGFP, both RANKL1-DsRed (Fig. 3*D*) and RANKL1-EGFP (Fig. 3*E*) were colocalized almost identically (Fig. 3*F*). In the cells cotransfected with RANKL1-DsRed and RANKL2-EGFP, both RANKL1-DsRed (Fig. 3*G*) and RANKL2-EGFP (Fig. 3*H*) were colocalized, but the identity was not as complete as RANKL1-DsRed and RANKL1-EGFP (Fig. 3*I*). Colocalizations of RANKL1-DsRed (Fig. 3*J*) and RANKL3-EGFP (Fig. 3*K*) and of RANKL2-DsRed (Fig. 3*M*) and

[2] T. Ikeda and J. Suzuki, unpublished data.

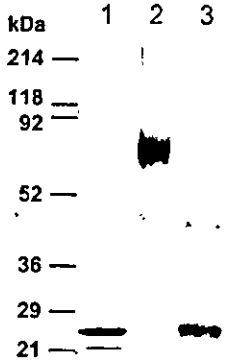

FIG. 2. **Cross-linking and the cleavage of RANKL3.** Recombinant mouse RANKL3 was cross-linked with EGS at 4 °C for 2 h, analyzed on SDS-PAGE, and visualized by Coomassie Brilliant Blue staining. The cross-linked sample was then cleaved by hydroxylamine hydrochloride. *Lanes 1–3* are uncross-linked (*lane 1*), cross-linked (*lane 2*) and cleaved after cross-linked (*lane 3*), respectively.

RANKL3-EGFP (Fig. 3*N*) were poorer, but in some regions of the cytoplasms of the cells, colocalized dots were detected (Fig. 3, *L* and *O*).

Functions of RANKL Isoforms on Osteoclastogenesis—We produced NIH3T3 cells expressing each RANKL isoform or different RANKL isoforms, and several clones for each transformant were used as stromal cells for *in vitro* osteoclastogenesis assay. In addition to macrophage colony-stimulating factor, 1α,25-dihydroxyvitamin D_3 and dexamethasone were further supplemented with the culture medium to down-regulate the expression of OPG of both NIH3T3 cells and macrophages (Fig. 4*A*). NIH3T3 cells expressing RANKL1 or RANKL2 induced TRAP-positive mononuclear preosteoclasts, but few multinucleated osteoclasts were formed (Fig. 4*B*, *a* and *b*). NIH3T3 cells expressing RANKL3 did not induce any TRAP-positive cells (Fig. 4*B*, *c*). NIH3T3 cells showing coexpression of RANKL1 and RANKL2 induced markedly expanded multinucleated osteoclasts. Most of the culture area was covered with the multinucleated osteoclasts, and few mononuclear TRAP-positive preosteoclasts were observed at 1 week after the coculture (Fig. 4*B*, *d*). NIH3T3 cells with coexpression of RANKL1 and RANKL3 and of RANKL2 and RANKL3 induced mononuclear TRAP-positive preosteoclasts, but the additional expression of RANKL3 did not change the number significantly (Fig. 4*B*, *e* and *f*, and 4*C*).

To elucidate whether the coexpression of RANKL1 and RANKL2 in the same cell is necessary to induce multinucleated osteoclasts, NIH3T3 cells expressing RANKL1 were mixed with the cells expressing RANKL2 and then used for coculture. Mixture of RANKL1-expressing cells and RANKL2-expressing cells induced mononuclear TRAP-positive preosteoclasts but did not induce multinucleated osteoclasts (Fig. 4*B*, *g*, and 4*D*). There is also a possibility that additional expression of the same RANKL isoform promotes the formation of multinucleated osteoclasts. To evaluate this, pcDNA3.1-RANKL1 or pcDNA3.1-RANKL2 was additionally transfected to cells showing the expression of RANKL1 or RANKL2, respectively. Additional expression of RANKL1 and additional expression of RANKL2 induced a few multinucleated osteoclasts (Fig. 4*B*, *h*, and data not shown). The expressions of RANKL1 in NIH3T3 cells used in the experiments shown in Fig. 4*B*, *a*, and 4*B*, *h*, are shown in Fig. 4*E*.

Previously, we reported that all the analyzed organs and a bone marrow stromal cell line ST2 expressed the three RANKL isoforms (13). Then, we further added the expression of RANKL3 in the NIH3T3 cells expressing RANKL1 and RANKL2 (Fig. 5, *A* and *B*). Additional expression of RANKL3

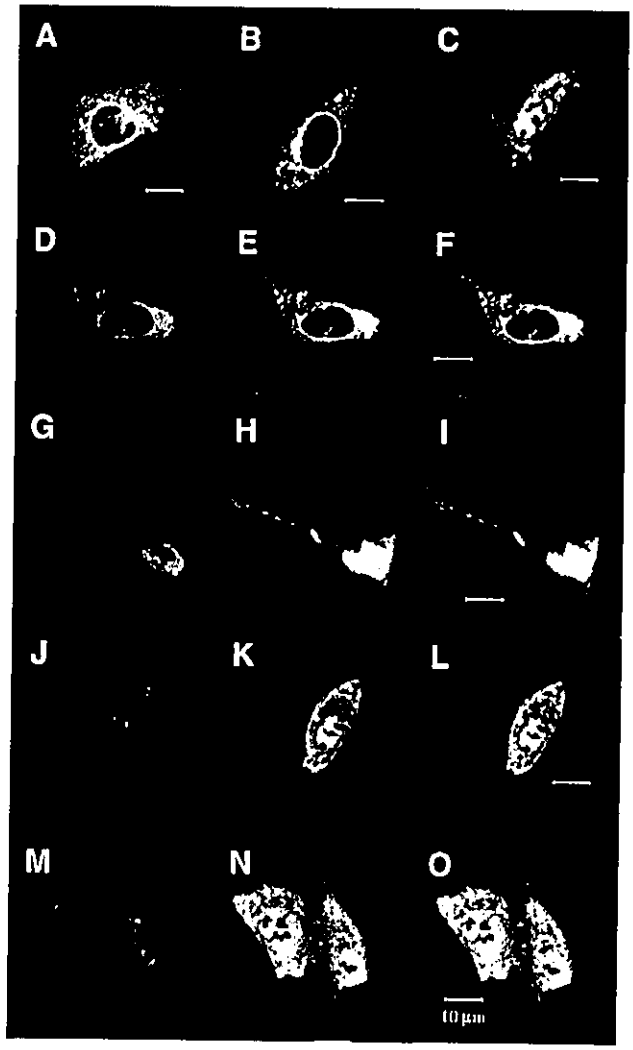

FIG. 3. **Confocal microscopy of NIH3T3 cells transfected with EGFP-tagged RANKL and cotransfected with DsRed-tagged RANKL and EGFP-tagged RANKL.** *A–C*, localization of each RANKL isoform. Localization of RANKL1-EGFP (*A*), RANKL2-EGFP (*B*), and RANKL3-EGFP (*C*) in transfected NIH3T3 cells is shown. *D–F*, NIH3T3 cells with the coexpression of RANKL1-DsRed and RANKL1-EGFP. Localization of RANKL1-DsRed (*D*) and RANKL1-EGFP (*E*) and their merged product (*F*) is shown. *G–I*, NIH3T3 cells with the coexpression of RANKL1-DsRed and RANKL2-EGFP. Localization of RANKL1-DsRed (*G*) and RANKL2-EGFP (*H*), and their merged product (*I*) is shown. *J–L*, NIH3T3 cells with the coexpression of RANKL1-DsRed and RANKL3-EGFP. Localization of RANKL1-DsRed (*J*) and RANKL3-EGFP (*K*) and their merged product (*L*) is shown. *M–O*, NIH3T3 cells with the coexpression of RANKL2-DsRed and RANKL3-EGFP. Localization of RANKL2-DsRed (*M*) and RANKL3-EGFP (*N*) and their merged product (*O*) is shown. *Bars*, 10 μm.

significantly decreased the formation of osteoclasts, and many unfused mononuclear TRAP-positive preosteoclasts were observed (Fig. 5*C*, *a* and *b*, and 5*D*).

The cocultures using NIH3T3 cells expressing RANKL1 and RANKL2 formed relatively large resorption lacunae on the dentin slices (Fig. 5*C*, *c*). On the dentin slices of the cocultures using NIH3T3 cells expressing RANKL1, RANKL2, and RANKL3, resorption lacunae were also formed, but the size was smaller (Fig. 5*C*, *d*). The area of the resorption lacunae on the dentin slices in the cocultures using NIH3T3 cells expressing RANKL1, RANKL2, and RANKL3 was significantly decreased as compared with that in the cocultures expressing RANKL1 and RANKL2 (Fig. 5*E*). To further analyze the effect

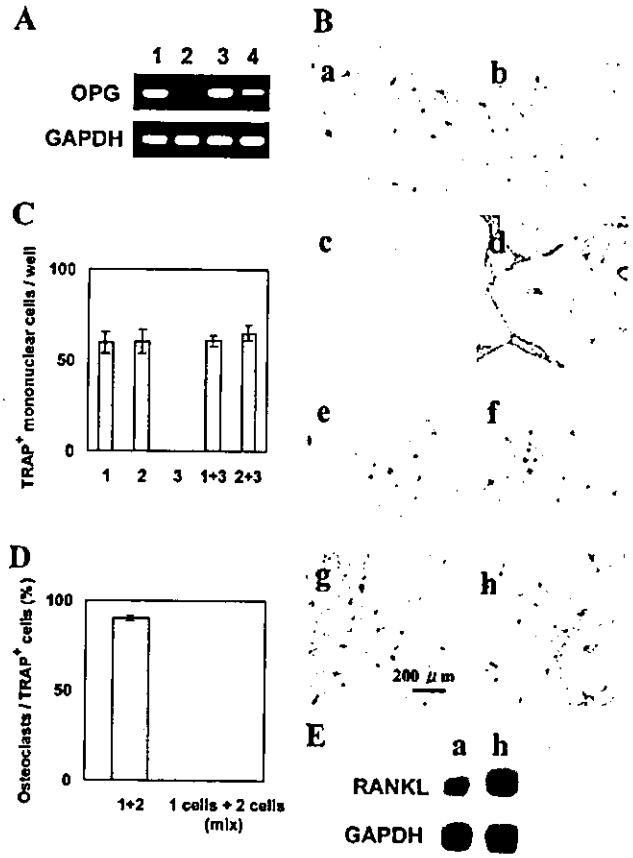

FIG. 4. **Effects of RANKL isoforms on TRAP-positive cell formation.** *A*, RT-PCR of OPG in the bone marrow macrophages (upper *lanes 1* and *2*) and NIH3T3 cells (*upper lanes 3* and *4*) with (*upper lanes 2* and *4*) or without (*upper lanes 1* and *3*) treatment of 1α,25-dihydroxyvitamin D_3 and dexamethasone. RT-PCR was performed using primers 5′-GGACAGTTTGCCTGGGACCAAAGTGAATGC-3′ and 5′-TGAAGCTGTGCAGGAACCTCATGGTCTTCC-3′ under the condition described under "Experimental Procedures." The *lower lanes* represent the expression of glyceraldehyde-3-phosphate dehydrogenese (*GAPDH*). *B*, cocultures of bone marrow macrophages and NIH3T3 cells expressing RANKL1 (*a*), RANKL2 (*b*), RANKL3 (*c*), RANKL1 and RANKL2 (*d*), RANKL1 and RANKL3 (*e*), and RANKL2 and RANKL3 (*f*). *g* shows coculture of bone marrow macrophages with a mixture of RANKL1-expressing NIH3T3 cells and RANKL2-expressing NIH3T3 cells. *h* shows cocultures of bone marrow macrophages and NIH3T3 cells cotransfected with pMIK HygB-RANKL1 and pcDNA3.1-RANKL1. *C* and *D*, effect of the expression of RANKL isoforms on the formation of preosteoclasts (*C*) and osteoclasts (*D*). *E*, Northern hybridization of the cells used in *panel B*, *a* and *h*, using the probes against mouse RANKL and glyceraldehyde-3-phosphate dehydrogenase. Cocultures were stained to detect the TRAP activity. Osteoclasts/TRAP+ cells (%) represent the percent of multinucleated osteoclasts/total TRAP-positive cells.

of RANKL3 on the phenotypes of osteoclasts, the presence of CT-Rs was analyzed by immunohistochemistry. In the cocultures of bone marrow macrophages and NIH3T3 cells expressing RANKL1, RANKL2, and RANKL3, CT-Rs were detected in both mononuclear and multinucleated cells (Fig. 5*C*, *e*) as reported previously in cocultures of mouse spleen cells and ST2 cells (5). In the cocultures analyzed with the anti-CT-Rs antibody preabsorbed with the blocking peptide, no CT-R-positive cell was found (Fig. 5*C*, *f*).

DISCUSSION

RANKL, a member of TNF, had been expected to form multimeric structures similar to TNF-α and TNF-β. Studies of sedimentation equilibrium analytical ultracentrifugation and crystallography showed that the extracellular domain of RANKL forms trimeric structures (17, 18, 23). On the other hand, we previously identified three isoforms of mouse RANKL cDNA. One was identical to the originally reported RANKL, another had a shorter intracellular domain, and the other lacked the intracellular and transmembrane domains, which were named RANKL1, RANKL2, and RANKL3, respectively (13). We hypothesized that these RANKL isoforms interact.

Here, we showed interactions of RANKL1 with RANKL1 or RANKL2 by immunoprecipitation using the proteins tagged with EGFP or DsRed (Fig. 1). However, RANKL3 did not precipitate with RANKL1 or RANKL2. Since RANKL3 has the complete extracellular domain of RANKL, RANKL3 may interact with RANKL isoforms as reported previously (17, 18, 23). Next, we showed that recombinant RANKL3 without the tag interacts and forms a trimer by a cross-linking study (Fig. 2). From these results, it was suggested that RANKL3 also interacts with other RANKL isoforms at the extracellular domain and forms homo- or heterotrimers, although we do not have direct evidence for multimerization of RANKL3 to RANKL1 and RANKL2. In addition, the findings suggest that the tagged proteins do not influence the multimerization of RANKL, and thus RANKL1 interacts with RANKL1 and RANKL2. Although interaction of RANKL1 with RANKL1 or RANKL2 was detected by immunoprecipitation, the interaction was suggested to be weak because the interaction was not seen when cells were lysed with the lysis buffer containing Nonidet P-40 and was only detected when one of the very mild detergents, digitonin, was used in place of Nonidet P-40. [3] Poorer colocalization of RANKL3 with RANKL1 or RANKL2 in the transfected cells (Fig. 3) suggests that the interaction of RANKL3 is still weaker than RANKL1 or RANKL2, and this might be the reason for the dissociation of RANKL3.

Localization of RANKL3 was different from those of RANKL1 and RANKL2 (Fig. 3), and the diffuse distribution of RANKL3 in the cytoplasmic region suggests that RANKL3 was not transported and secreted adequately, and accumulated in the cytoplasmic region. This might be true because in the cocultures using NIH3T3 cells expressing RANKL3, neither preosteoclasts nor osteoclasts were formed (Fig. 4*B*, *c*), although recombinant RANKL3 protein induced osteoclasts when administered to bone marrow macrophages.[2] However, there is also a possibility that RANKL3 is secreted as a soluble form protein, but it diffuses in the culture medium, and the final concentration is not sufficient to induce preosteoclasts or osteoclasts.

Coexpression of RANKL1 and RANKL2 markedly enhanced the formation of multinucleated osteoclasts, but a mixture of RANKL1-expressing cells and RANKL2-expressing cells did not. These findings suggest that the coexpression of both RANKL1 and RANKL2 in the same cells is important for the formation of multinucleated osteoclasts. As shown in Figs. 1 and 2, RANKL isoforms interact with one another, and the coexpression is suggested to form heteromultimers of RANKL1 and RANKL2. However, overexpression of RANKL1 or RANKL2 also induced multinucleated osteoclasts. These results suggest that heteromultimers of RANKL1 and RANKL2 markedly stimulate fusion of preosteoclasts in this assay system, but they are not essential to fusion of preosteoclasts, and these results also suggest that higher expression of RANKL1 or RANKL2 is necessary for fusion than formation of preosteoclasts.

As described above, RANKL3 induced neither preosteoclasts nor osteoclasts, and the additional expression of RANKL3 to RANKL1 or RANKL2 did not change the formation of preosteoclasts (Fig. 4*B*, *e* and *f*, and 4*C*). However, the expression of

[3] M. Kasai and T. Ikeda, unpublished data.

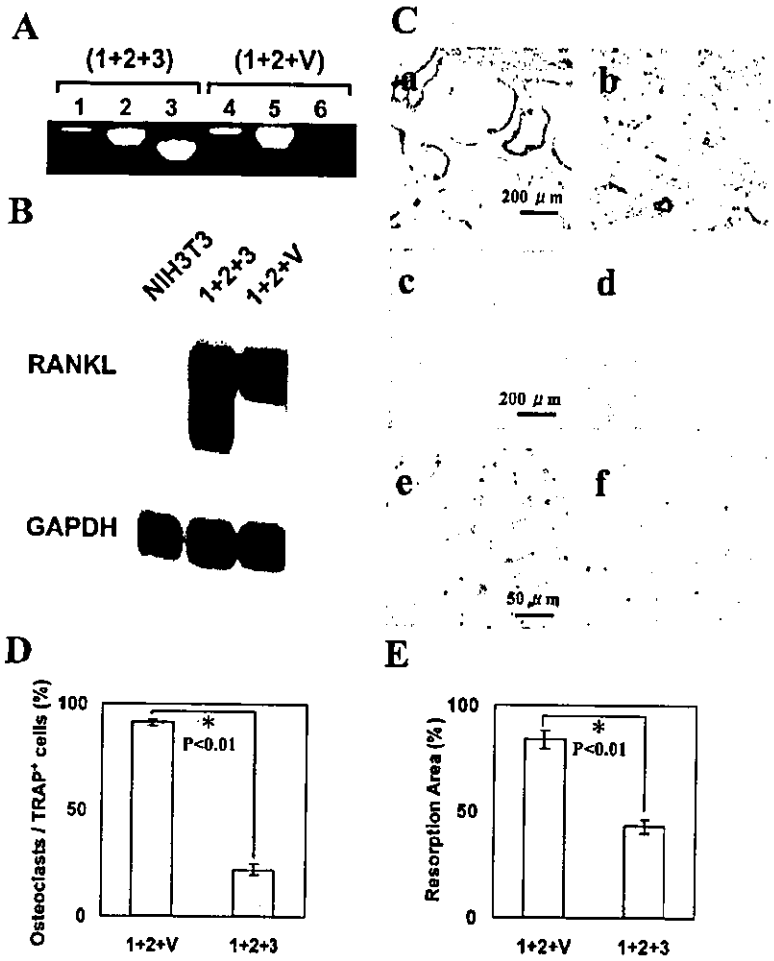

FIG. 5. **Coexpression of RANKL3 with RANKL1 and RANKL2 inhibits osteoclastogenesis.** *A*, RT-PCR of NIH-3T3 cells transfected with pMIK HygB-RANKL1, pcDNA3.1-RANKL2 and pEFBOSbsr-RANKL3 (1 + 2 + 3), and NIH3T3 cells transfected with pMIK HygB-RANKL1, pcDNA3.1-RANKL2, and pEFBOSbsr vector (1 + 2 + v). *Lanes 1–3* show detection of RANKL1 (*1*), RANKL2 (*2*), and RANKL3 (*3*), respectively. *B*, Northern hybridization of the cells described in *A* and control NIH3T3 cells using the probe against mouse RANKL. *GAPDH*, glyceraldehyde-3-phosphate dehydrogenese. *C*, cocultures of bone marrow macrophages and NIH3T3 cells expressing RANKL1 and RANKL2, which were further transfected with an additional expression vector, pEFBOSbsr (*a*), and NIH3T3 cells expressing RANKL1, RANKL2, and RANKL3 (*b*). Cocultures were stained to detect the TRAP activity. Formation of resorption lacunae by the coculture was shown in *A* (*c*) and in *B* (*d*). Immunohistochemistry of CT-Rs in the coculture of bone marrow macrophages and NIH3T3 cells expressing RANKL1, RANKL2, and RANKL3 is shown. The cocultures treated with anti-CT-Rs antibody (*e*) and the preabsorbed antibody (*f*) are shown. *D*, effect of the coexpression of RANKL3 with RANKL1 and RANKL2 on osteoclastogenesis. Osteoclasts/TRAP+ cells (%) represent the percent of multinucleated osteoclasts/total TRAP-positive cells. *E*, effect of the coexpression of RANKL3 with RANKL1 and RANKL2 on formation of resorption lacunae. *Resorption Area* (%) represents the percentage of the area of resorption lacunae/area of the dentin slice.

RANKL3 significantly decreased the percent of multinucleated osteoclasts/total TRAP-positive cells when coexpressed with RANKL1 and RANKL2. These results suggest that RANKL3 specifically inhibits fusion of preosteoclasts when coexpressed with RANKL1 and RANKL2. Considering the multimerization of RANKL isoforms, the mechanism to inhibit the fusion of preosteoclasts by the expression of RANKL3 might be associated with intracellular interactions of RANKL3 with RANKL1 and/or RANKL2. As shown in Fig. 5*C*, *e*, the expression of CT-Rs was detected in preosteoclasts and osteoclasts induced by NIH3T3 cells expressing RANKL1, RANKL2, and RANKL3. These findings confirm that the expression of RANKL3 does not affect phenotypes of preosteoclasts and osteoclasts but inhibits only fusion of preosteoclasts.

The findings in the present study strongly suggest that multiple multimeric structures of RANKL are present and regulate bone metabolism. Drugs with selectable regulation of the expression of each RANKL isoform may work as regulators of bone metabolism. Furthermore, RANKL has multiple functions throughout osteoclastogenesis: differentiation and fusion of osteoclast progenitor cells and activation and survival of osteoclasts (24–27). A part of these multiple functions may be expressed by the multiple multimeric structures of RANKL.

Acknowledgments—We thank Dr. N. Udagawa for generously providing dentin slices and discussion, Dr. M. Tatsumi for generously providing pEFBOSbsr vector, and Dr. H. Yamato and H. Murkami for instruction to quantify resorption lacunae. We also thank N. Ishida for technical support.

REFERENCES

1. Nakagawa, N., Kinosaki, M., Yamaguchi, K., Yasuda, H., Yano, K., Morinaga, T., and Higashio, K. (1998) *Biochem. Biophys. Res. Commun.* 253, 395–400
2. Hsu, H., Lacey, D. L., Dunstan, C. R., Solovyev, I., Colombero, A., Timms, E., Tan, H.-L., Elliott, G., Kelley, M. J., Sarosi, I., Wang, L., Xia, X. Z., Elliott, R., Chiu, L., Black, T., Scully, S., Capparelli, C., Morony, S., Shimamoto, G., Bass, M. B., and Boyle, W. J. (1999) *Proc. Natl. Acad. Sci. U. S. A.* 96, 3540–3545
3. Simonet, W. S., Lacey, D. L., Dunstan, C. R., Kelley, M., Chang, M.-S., Lüthy, R., Nguyen, H. Q., Wooden, S., Bennett, L., Boone, T., Shimamoto, G., DeRose, M., Elliott, R., Colombero, A., Tan, H.-L., Trail, G., Sullivan, J., Davy, E., Bucay, N., Renshaw-Gegg, L., Hughes, T. M., Hill, D., Pattison, W., Campbell, P., Sander, S., Van, G., Tarpley, J., Derby, P., Lee, R., and Boyle, W. J. (1997) *Cell* 89, 309–319
4. Yasuda, H., Shima, N., Nakagawa, N., Mochizuki, S., Yano, K., Fujise, N., Sato, Y., Goto, M., Yamaguchi, K., Kuriyama, M., Kanno, T., Murakami, A., Tsuda, E., Morinaga, T., and Higashio, K. (1998) *Endocrinology* 139, 1329–1337
5. Udagawa, N., Takahashi, N., Akatsu, T., Sasaki, T., Yamaguchi, A., Kodama, H., Martin, J., and Suda, T. (1989) *Endocrinology* 125, 1805–1813
6. Tsukii, K., Shima, N., Mochizuki, S., Yamaguchi, K., Kinosaki, M., Yano, K., Shibata, O., Udagawa, N., Yasuda, H., Suda, T., and Higashio, K. (1998) *Biochem. Biophys. Res. Commun.* 246, 337–341
7. Lacey, D. L., Timms, E., Tan, H.-L., Kelley, M. J., Dunstan, C. R., Burgess, T., Elliott, R., Colombero, A., Elliott, G., Scully, S., Hsu, H., Sullivan, J., Hawkins, N., Davy, E., Capparelli, A., Eli, Y.-X., Qian, S., Kaufman, I., Sarosi, V., Shalhoub, G., Senaldi, J., Guo, J., Delaney, C., and Boyle, W. J. (1998) *Cell* 93, 165–1176
8. Yasuda, H., Shima, N., Nakagawa, N., Yamaguchi, K., Kinosaki, M., Mochizuki, S., Tomoyasu, A., Yano, K., Goto, M., Murakami, A., Tsuda, E., Morinaga, T., Higashio, K., Udagawa, N., Takahashi, N., and Suda, T. (1998) *Proc. Natl. Acad. Sci. U. S. A.* 95, 3597–3600
9. Lum, L., Wong, B. R., Josien, R., Becherer, J. D., Erdjument-Bromage, H., Schlöndorff, J., Tempst, P., Choi, Y., and Blobel, C. P. (1999) *J. Biol. Chem.* 274, 13613–13618
10. Kong, Y. Y., Yoshida, H., Sarosi, I., Tan, H.-L., Timms, E., Capparelli, C., Morony, S., Oliveira-dos-Santos, A. J., Van, G., Itie, A., Khoo, W., Wakeham, A., Dunstan, C. R., Lacey, D. L., Mak, T. W., Boyle, W. J., and Penninger, J. M. (1999) *Nature* 397, 315–323

11. Dougall, W. C., Glaccum, M., Charrier, K., Rohrbach, K., Brasel, K., Smedt, T. D., Daro, E., Smith, J., Tometsko, M. E., Maliszewski, C. R., Armstrong, A., Shen, V., Bain, S., Cosman, D., Anderson, D., Morrissey, P. J., Peschon, J. J., and Schuh, J. (1999) *Genes Dev.* **13**, 2412–2424
12. Li, J., Sarosi, I., Yan, X.-Q., Morony, S., Capparelli, C., Tan, H.-L., McCabe, S., Elliott, R., Scully, S., Van, G., Kaufman, S., Juan, S.-C., Sun, Y., Tarpley, J., Martin, L., Christensen, K., McCabe, J., Kostenuik, P., Hsu, H., Fletcher, F., Dunstan, C. R., Lacey, D. L., and Bolye, W. J. (2000) *Proc. Natl. Acad. Sci. U. S. A.* **97**, 1566–1571
13. Ikeda, T., Kasai, M., Utsuyama, M., and Hirokawa, K. (2000) *Endocrinology* **142**, 1419–1426
14. Smith, R. A., and Baglioni, C. (1987) *J. Biol. Chem.* **262**, 6951–6954
15. Jones, E. Y., Stuart, D. I., and Walker, N. P. (1989) *Nature* **338**, 225–228
16. Banner, D. W., D'Arcy, A., Janes, W., Gents, R., Schoenfeld, H. J., Broger, C., Loetscher, H., and Lesslauer, W. (1993) *Cell* **73**, 431–445
17. Ito, S., Wakabayashi, K., Ubukata, O., Hayashi, S., Okada, F., and Hata, T. (2002) *J. Biol. Chem.* **277**, 6631–6636
18. Lam, J., Nelson, C. A., Ross, F. P., Teitelbaum, S. L., and Fremont, D. H. (2001) *J. Clin. Invest.* **108**, 971–979
19. Hachiya, A., Aizawa, S., Tanaka, M., Takahashi, Y., Ida, S., Gatanaga, H., Hirabayashi, Y., Kojima, A., Tatsumi, M., and Oka, S. (2001) *Antimicrob. Agents Chemother.* **45**, 495–501
20. Shioi, A., Ross, F. P., and Teitelbaum, S. L. (1994) *Calcif. Tissue Int.* **55**, 387–394
21. Inoue, M., Namba, N., Chappel, J., Teitelbaum, S. L., and Ross, F. P. (1998) *Mol. Endocrinol.* **12**, 1955–1962
22. Yamato, H., Okazaki, R., Ishii, T., Ogata, E., Sato, T., Kumegawa, M., Akaogi, K., Taniguchi, N., and Matsumoto, T. (1993) *Calcif. Tissue Int.* **52**, 255–260
23. Willard, D., Chen, W. J., Barrett, G., Blackburn, K., Bynum, J., Consler, T., Hoffman, C., Horne, E., Iannone, M. A., Kadwell, S., Parham, J., and Ellis, B. (2000) *Protein Expression Purif.* **20**, 48–57
24. Fuller, K., Wong, B., Fox, S., Choi, Y., and Chambers, T. J. (1998) *J. Exp. Med.* **188**, 997–1001
25. Burgess, T. L., Qian, Y.-X., Kaufman, S., Ring, B. D., Van, G., Caparelli, C., Kelley, M., Hsu, H., Boyle, W. J., Dunstan, C. R., Hu, S., and Lacey, D. L. (1999) *J. Cell Biol.* **145**, 527–538
26. Jimi, E., Akiyama, S., Tsurukai, T., Okahashi, N., Kobayashi, K., Udagawa, N., Nishihara, T., Takahashi, N., and Suda, T. (1999) *J. Immunol.* **163**, 434–442
27. Lacey, D. L., Tan, H.-L., Lu, J., Kaufman, S., Van, G., Qiu, W., Rattan, A., Scully, S., Fletcher, F., Juan, T., Kelley, M., Burgess, T. L., Boyle, W. J., and Polverino, A. J. (2000) *Am. J. Pathol.* **157**, 435–448

JOURNAL OF BONE AND MINERAL RESEARCH
Volume 16, Number 8, 2001

Expression Profiles of Receptor Activator of Nuclear Factor κB Ligand, Receptor Activator of Nuclear Factor κB, and Osteoprotegerin Messenger RNA in Aged and Ovariectomized Rat Bones

TOHRU IKEDA,[1] MASANORI UTSUYAMA,[1,2] and KATSUIKU HIROKAWA[1]

ABSTRACT

The receptor activator of nuclear factor-κB ligand (RANKL; also known as tumor necrosis factor–related activation-induced cytokine [TRANCE], osteoprotegerin ligand [OPGL], and osteoclast differentiation factor [ODF]) is a transmembrane ligand expressed in osteoblasts and bone marrow stromal cells. It binds to RANK, which is expressed in osteoclast progenitor cells, and induces osteoclastogenesis. OPG, a decoy receptor for RANKL, also binds to RANKL, and competitive binding of RANKL with RANK or OPG is thought to regulate bone metabolism. To investigate roles of the RANKL/RANK/OPG system in pathophysiological conditions, the expression of RANKL, RANK, and OPG messenger RNA (mRNA) was analyzed in bones of aged and ovariectomized rats by means of in situ hybridization. In the control 8-week-old male and sham-operated female rat bones, the expression of RANKL mRNA was detected in hypertrophic chondrocytes of the growth plate and some periosteal and endosteal mesenchymal cells. The expression of RANK mRNA was detected in osteoclast-like cells and mononuclear cells in contact with the cortical and trabecular bones. The expression of OPG mRNA was detected in proliferating chondrocytes and osteocytes. In the 2.5-year-old rat bones, the expression of RANKL, RANK, and OPG mRNA tended to decrease except for the endosteal region. In the ovariectomized rat bones, the expression of RANKL, RANK, and OPG mRNA increased, and high expression of OPG mRNA was induced in resting chondrocytes and osteocytes. These results suggest that estrogen deficiency stimulates the RANKL/RANK/OPG system and induces OPG in cells that have been thought to be less important for bone metabolism. (J Bone Miner Res 2001;16:1416–1425)

Key words: **receptor activator of nuclear factor κB ligand, receptor activator of nuclear factor κB, osteoprotegerin, aging, ovariectomy**

INTRODUCTION

Discovery of the receptor activator of nuclear factor κB ligand (RANKL, also called osteoprotegerin ligand [OPGL]/osteoclast differentiation factor [ODF]/tumor necrosis factor [TNF]–related activation-induced cytokine [TRANCE]) clarified the molecular mechanisms behind the initial steps of osteoclastogenesis.[1–7] RANKL is a type II TNF-like transmembrane protein, which binds to the receptor activator of nuclear factor κB (NF-κB; RANK) or OPG. RANK is expressed in osteoclast progenitor cells and induces osteoclastogenesis by binding to RANKL.[5,7,8] OPG

[1]Department of Pathology and Immunology, Aging and Developmental Science, Graduate School, Tokyo Medical and Dental University, Bunkyo-ku, Tokyo, Japan.
[2]Department of Membrane Biochemistry, Tokyo Metropolitan Institute of Gerontology, Itabashi-ku, Tokyo, Japan.